Symmetries of spatial correlators of light and heavy mesons in high temperature lattice QCD

Ting-Wai Chiu[1, 2, 3, 4, *]

[1]*Department of Physics, National Taiwan Normal University,*
Taipei, Taiwan 11677, Republic of China

[2]*Institute of Physics, Academia Sinica, Taipei, Taiwan 11529, Republic of China*

[3]*Physics Division, National Center for Theoretical Sciences,*
Taipei, Taiwan 10617, Republic of China

[4]*Center for Theoretical Physics, Department of Physics, National Taiwan University,*
Taipei, Taiwan 10617, Republic of China

Abstract

The spatial z-correlators of meson operators in $N_f = 2+1+1$ lattice QCD with optimal domain-wall quarks at the physical point are studied for seven temperatures in the range of 190-1540 MeV. The meson operators include a complete set of Dirac bilinears (scalar, pseudoscalar, vector, axial vector, tensor vector, and axial-tensor vector), and each for six flavor combinations ($\bar{u}d$, $\bar{u}s$, $\bar{s}s$, $\bar{u}c$, $\bar{s}c$, and $\bar{c}c$). In Ref. [1], we focused on the meson correlators of u and d quarks, and discussed their implications for the effective restoration of $SU(2)_L \times SU(2)_R$ and $U(1)_A$ chiral symmetries, as well as the emergence of approximate $SU(2)_{CS}$ chiral spin symmetry. In this work, we extend our study to meson correlators of six flavor contents, and first observe the hierarchical restoration of chiral symmetries in QCD, from $SU(2)_L \times SU(2)_R \times U(1)_A$ to $SU(3)_L \times SU(3)_R \times U(1)_A$, and to $SU(4)_L \times SU(4)_R \times U(1)_A$, as the temperature is increased from 190 MeV to 1540 MeV. Moreover, we compare the temperature windows for the emergence of the approximate $SU(2)_{CS}$ symmetry in light and heavy vector mesons, and find that the temperature windows are dominated by the $(\bar{u}c, \bar{s}c, \bar{c}c)$ sectors.

I. Introduction

Understanding the nature of strongly interacting matter at high temperatures is crucial for uncovering the mechanisms governing matter creation in the early universe and elucidating the outcomes of relativistic heavy ion collision experiments such as those at LHC and RHIC, as well as those of electron ion collision experiments at the planned electron-ion colliders. A first step in this pursuit is to find out the symmetries in Quantum Chromodynamics (QCD) at high temperatures, which are essential in determining the properties and dynamics of matter under extreme conditions.

First, consider QCD with N_f massless quarks. Its action possesses the $SU(N_f)_L \times SU(N_f)_R \times U(1)_A$ chiral symmetry. At low temperatures $T < T_c^0$ (where T_c^0 depends on N_f, and the superscript "0" denotes zero quark mass), quarks and gluons are confined in hadrons, and the $SU(N_f)_L \times SU(N_f)_R$ chiral symmetry is spontaneously broken down to $SU(N_f)_V$ by the vacuum of QCD, with nonzero chiral condensate. Moreover, the $U(1)_A$ axial symmetry

---

* twchiu@phys.ntu.edu.tw

is explicitly broken by the chiral anomaly, due to the quantum fluctuations of topologically nontrivial gauge fields. As the temperature is increased above T_c^0, the chiral condensate becomes zero, and the $SU(N_f)_L \times SU(N_f)_R$ chiral symmetry is restored. Furthermore, the $U(1)_A$ axial symmetry is effectively restored at $T \gtrsim T_1^0 \gtrsim T_c^0$, due to the suppression of the quantum fluctuations of topologically nontrivial gauge configurations at high temperatures. So far, it is still an open question whether $T_1^0 > T_c^0$ or $T_1^0 \simeq T_c^0$. Here we define T_{c1}^0 to be the maximum of T_c^0 and T_1^0,

$$T_{c1}^0 \equiv \max(T_c^0, T_1^0), \tag{1}$$

such that the theory possesses the $SU(N_f)_L \times SU(N_f)_R \times U(1)_A$ chiral symmetry for $T > T_{c1}^0$.

Next, consider QCD with physical (u, d, s, c, b) quarks. Its action does not possess the $SU(N)_L \times SU(N)_R \times U(1)_A$ chiral symmetry for any integer N from 2 to 5, due to the explicit breakings of the nonzero quark masses. However, as T is increased successively, each quark acquires thermal energy of the order of πT, and eventually its rest mass energy becomes negligible when $\pi T \gg m_q$. Also, since the quark masses range from a few MeV to a few GeV, it follows that as the temperature is increased successively, the chiral symmetry is restored hierarchically from $SU(2)_L \times SU(2)_R \times U(1)_A$ of (u, d) quarks to $SU(3)_L \times SU(3)_R \times U(1)_A$ of (u, d, s) quarks, then to $SU(4)_L \times SU(4)_R \times U(1)_A$ of (u, d, s, c) quarks, and finally to $SU(5)_L \times SU(5)_R \times U(1)_A$ of (u, d, s, c, b) quarks. Since the restoration of chiral symmetries is manifested by the degeneracies of meson z-correlators (as well as other observables), we can use the splittings of the meson z-correlators of the symmetry multiplets to examine the realization of the hierarchical restoration of chiral symmetries in high temperature QCD. Strictly speaking, these chiral symmetries should be regarded as "emergent" symmetries rather than "restored" symmetries, since the QCD action with physical quark masses does not possess chiral symmetries at all. In the following, it is understood that "restoration of chiral symmetries" stands for "emergence of chiral symmetries". Similar to (1), we define

$$T_{c1}^{\bar{q}Q} \equiv \max(T_c^{\bar{q}Q}, T_1^{\bar{q}Q}), \tag{2}$$

where $T_c^{\bar{q}Q}$ ($T_1^{\bar{q}Q}$) is the temperature for the manifestation of $SU(2)_L \times SU(2)_R$ ($U(1)_A$) chiral symmetry via the meson z-correlators with flavor content $\bar{q}Q$. Then, for $T > T_{c1}^{\bar{q}Q}$, the theory possesses the $SU(2)_L \times SU(2)_R \times U(1)_A$ chiral symmetry of the $\bar{q}Q$ sector.

Note that since 1987 [2], there have been many lattice studies using the screening masses of meson z-correlators to investigate the effective restoration of $U(1)_A$ and $SU(2)_L \times SU(2)_R$ chiral symmetries of u and d quarks in high temperature QCD, see, e.g., Ref. [3] and references therein. However, so far, there seems no discussions in the literature about the hierarchical restoration of chiral symmetries in high temperature QCD, except for a brief mention in Ref. [1].

In this work, we investigate the hierarchical restoration of chiral symmetries in $N_f = 2+1+1$ lattice QCD with optimal domain-wall quarks at the physical point. We first observe the hierarchical restoration of chiral symmetries from $SU(2)_L \times SU(2)_R \times U(1)_A$ of (u, d) quarks, to $SU(3)_L \times SU(3)_R \times U(1)_A$ of (u, d, s) quarks, and finally to $SU(4)_L \times SU(4)_R \times U(1)_A$ of (u, d, s, c) quarks, as the temperature is increased from 190 MeV to 1540 MeV. We compute the meson z-correlators for a complete set of Dirac bilinears (scalar, pseudoscalar, vector, axial vector, tensor vector, and axial-tensor vector), and each for six combinations of quark flavors ($\bar{u}d$, $\bar{u}s$, $\bar{s}s$, $\bar{u}c$, $\bar{s}c$, and $\bar{c}c$). Then we use the degeneracies of meson z-correlators to investigate the hierarchical restoration of chiral symmetries in high temperature QCD.

The relationship between the $SU(2)_L \times SU(2)_R$ and $U(1)_A$ chiral symmetries and the degeneracy of meson z-correlators for (u, d) quarks in $N_f = 2 + 1 + 1$ QCD has been outlined in Ref. [1], and we follow the same conventions/notations therein. In this study, following Ref. [1], we also neglect the disconnected diagrams in the meson z-correlators. With this approximation, one can straightforwardly deduce the relationship between the $SU(N)_L \times SU(N)_R$ and $U(1)_A$ chiral symmetries of N ($2 \leq N \leq N_f$) quarks and the degeneracy of meson z-correlators, in QCD with N_f quarks, as follows. The restoration of $SU(N)_L \times SU(N)_R$ chiral symmetry of N quarks is manifested by the degeneracies of meson z-correlators in the vector and axial-vector channels, $C_{V_k}^{\bar{q}_i q_j}(z) = C_{A_k}^{\bar{q}_i q_j}(z)$, ($k = 1, 2, 4$), for *all* flavor combinations ($\bar{q}_i q_j$, $i, j = 1, \cdots, N$). The effective restoration of the $U(1)_A$ symmetry of N quarks is manifested by the degeneracies of meson z-correlators in the pseudoscalar and scalar channels, $C_P^{\bar{q}_i q_j}(z) = C_S^{\bar{q}_i q_j}(z)$, as well as in the tensor vector and axial-tensor vector channels, $C_{T_k}^{\bar{q}_i q_j}(z) = C_{X_k}^{\bar{q}_i q_j}(z)$, ($k = 1, 2, 4$), for *all* flavor combinations ($\bar{q}_i q_j$, $i, j = 1, \cdots, N$). At this point, we recall the studies of the symmetries and meson correlation functions in high temperature QCD with N_f massless quarks [4, 5], in which one the salient results is that the correlator of the flavor non-singlet pseudoscalar meson $\bar{q}\gamma_5 \lambda_a q$ is equal to that of

4

the flavor singlet pseudoscalar meson $\bar{q}\gamma_5 q$, for QCD with $N_f > 2$ at $T > T_c$. This implies that the disconnected diagrams do not have contributions to meson z-correlators in QCD with $N_f > 2$ massless quarks at $T > T_c$. However, at this moment, it is unknown to what extent the disconnected diagrams are suppressed in QCD with $N_f = 2+1(+1)(+1)$ physical quarks. We will address this question with noise estimation of all-to-all quark propagators, and will report our results in the future.

Besides the hierarchical restoration of chiral symmetries, we are also interested in the question whether there are any (approximate) emergent symmetries which are not the symmetries of the entire QCD action but only a part of it, e.g., the $SU(2)_{CS}$ chiral spin symmetry (with $U(1)_A$ as a subgroup) [6, 7], which is only a symmetry of chromoelectric part of the quark-gluon interaction, and also the color charge. Since the free fermions as well as the chromomagetic part of the quark-gluon interaction do not possess the $SU(2)_{CS}$ symmetry, its emergence in high temperature QCD suggests the possible existence of hadron-like objects which are predominantly bound by chromoelectric interactions. The $SU(2)_{CS}$ symmetry was first observed to manifest approximately in the multiplets of z-correlators of vector mesons, at temperatures $T \sim 220 - 500$ MeV in $N_f = 2$ lattice QCD with domain-wall fermions [8]. In Ref. [1], we studied the emergence of $SU(2)_{CS}$ chiral-spin symmetry in $N_f = 2+1+1$ lattice QCD with optimal domain-wall quarks at the physical point, and found that the $SU(2)_{CS}$ symmetry breaking in $N_f = 2+1+1$ lattice QCD is larger than that in $N_f = 2$ lattice QCD at the same temperature, for both z-correlators and t-corralators of vector mesons of u and d quarks. In this paper, we extend our study to vector meson z-correlators of all flavor combinations ($\bar{u}d$, $\bar{u}s$, $\bar{s}s$, $\bar{u}c$, $\bar{s}c$, $\bar{c}c$) in $N_f = 2+1+1$ lattice QCD at the physical point, and compare the emergence of approximate $SU(2)_{CS}$ chiral spin symmetry between different flavor sectors.

The outline of this paper is as follows. In Sec. II, the hybrid Monte-Carlo simulation of $N_f = 2+1+1$ lattice QCD with optimal domain-wall quarks at the physical point is briefly outlined, and the essential features and parameters of the seven gauge ensembles for this study are summarized. In Sec. III, the symmetry-breaking parameters for measuring the precision of various symmetries with the splittings of the z-correlators of the symmetry partners are defined. The results of meson z-correlators for six flavor combinations and seven temperatures in the range of 190-1540 MeV are presented in Sec. IV, while

the corresponding results of symmetry-breaking parameters are presented in Sec. V. The realization of hierarchical restoration of chiral symmetries in $N_f = 2 + 1 + 1$ QCD, from $SU(2)_L \times SU(2)_R \times U(1)_A$ to $SU(3)_L \times SU(3)_R \times U(1)_A$, and to $SU(4)_L \times SU(4)_R \times U(1)_A$, as the temperature is increased from 190 MeV to 1540 MeV, is demonstrated in Sec. V A. The temperature windows for the approximate $SU(2)_{CS}$ symmetry of six flavor combinations are presented in Sec. V B, which reveal the dominance of heavy vector meson channels of $(\bar{u}c, \bar{s}c, \bar{c}c)$ sectors. In Sec. VI, we conclude with some remarks.

II. Gauge ensembles

The gauge ensembles in this study are generated by hybrid Monte-Carlo (HMC) simulation of lattice QCD with $N_f = 2 + 1 + 1$ optimal domain-wall quarks [9] at the physical point, on the $32^3 \times (16, 12, 10, 8, 6, 4, 2)$ lattices, with the plaquette gauge action at $\beta = 6/g^2 = 6.20$. This set of ensembles are generated with the same actions [10, 11] and alogrithms as their counterparts on the $64^3 \times (20, 16, 12, 10, 8, 6)$ lattices [12], but with one-eighth of the spatial volume. The simulations are performed on a GPU cluster with various Nvidia GPUs. For each ensemble, after the initial thermalization, a set of gauge configurations are sampled and distributed to 16-32 simulation units, and each unit performed an independent stream of HMC simulation. For each HMC stream, one configuration is sampled every 5 trajectories. Finally collecting all sampled configurations from all HMC streams gives the total number of configurations of each ensemble. The lattice parameters and statistics of the gauge ensembles for computing the meson z-correlators in this study are summarized in Table I. The temperatures of these six ensembles are in the range $\sim 190 - 1540$ MeV, all above the pseudocritical temperature $T_c \sim 150$ MeV.

The lattice spacing and the $(u/d, s, c)$ quark masses are determined on the the $32^3 \times 64$ lattices with 427 configurations. The lattice spacing is determined using the Wilson flow [13, 14] with the condition $\{t^2 \langle E(t) \rangle\}|_{t=t_0} = 0.3$ and the input $\sqrt{t_0} = 0.1416(8)$ fm [15]. The physical $(u/d, s, c)$ quark masses are obtained by tuning their masses such that the masses of the lowest-lying states extracted from the time-correlation functions of the meson operators $\{\bar{u}\gamma_5 d, \bar{s}\gamma_i s, \bar{c}\gamma_i c\}$ are in good agreement with the physical masses of $\pi^{\pm}(140)$, $\phi(1020)$, and $J/\psi(3097)$.

TABLE I. The lattice parameters and statistics of the seven gauge ensembles for computing the meson correlators. The last 3 columns are the residual masses of u/d, s, and c quarks.

β	a[fm]	N_x	N_t	$m_{u/d}a$	$m_s a$	$m_c a$	T[MeV]	N_{confs}	$(m_{u/d}a)_{\text{res}}$	$(m_s a)_{\text{res}}$	$(m_c a)_{\text{res}}$
6.20	0.0641	32	16	0.00125	0.040	0.550	192	591	$1.9(2) \times 10^{-5}$	$1.5(2) \times 10^{-5}$	$4.3(7) \times 10^{-6}$
6.20	0.0641	32	12	0.00125	0.040	0.550	257	514	$1.9(2) \times 10^{-5}$	$1.6(1) \times 10^{-5}$	$3.8(5) \times 10^{-6}$
6.20	0.0641	32	10	0.00125	0.040	0.550	308	481	$5.7(7) \times 10^{-6}$	$5.1(6) \times 10^{-6}$	$1.4(2) \times 10^{-6}$
6.20	0.0641	32	8	0.00125	0.040	0.550	385	468	$6.3(9) \times 10^{-6}$	$6.0(7) \times 10^{-6}$	$3.0(9) \times 10^{-6}$
6.20	0.0641	32	6	0.00125	0.040	0.550	513	431	$5.8(9) \times 10^{-6}$	$5.6(8) \times 10^{-6}$	$3.4(7) \times 10^{-6}$
6.20	0.0641	32	4	0.00125	0.040	0.550	770	991	$1.2(2) \times 10^{-6}$	$1.2(2) \times 10^{-6}$	$1.2(2) \times 10^{-6}$
6.20	0.0641	32	2	0.00125	0.040	0.550	1540	770	$8.0(5) \times 10^{-7}$	$7.8(5) \times 10^{-7}$	$8.2(5) \times 10^{-7}$

The chiral symmetry breaking due to finite $N_s = 16$ (in the fifth dimension) can be measured by the residual mass of each quark flavor [16], as given in the last three columns of Table I. The residual masses of $(u/d, s, c)$ quarks are less than $(1.5\%, 0.04\%, 0.001\%)$ of their bare masses, amounting to less than $(0.06, 0.05, 0.02)$ MeV/c^2 respectively. This asserts that the chiral symmetry is well preserved such that the deviation of the bare quark mass m_q is sufficiently small in the effective 4D Dirac operator of optimal domain-wall fermion, for both light and heavy quarks. In other words, the chiral symmetry in the simulations are sufficiently precise to guarantee that the hadronic observables (e.g., meson correlators) can be evaluated to high precision, with the associated uncertainty much less than those due to statistics and other systematics.

III.   Symmetry breaking parameters

In order to give a quantitative measure for the manifestation of symmetries from the degeneracy of meson z-correlators with flavor content $\bar{q}Q$, we consider the symmetry breaking parameters as follows. To this end, we write the meson z-correlators as functions of the dimensionaless variable

$$zT = (n_z a)/(N_t a) = n_z/N_t, \tag{3}$$

where T is the temperature.

In general, the degeneracy of any two meson z-correlators $C_A(zT)$ and $C_B(zT)$ with flavor content $\bar{q}Q$ (where subscripts A and B denote their Dirac matrices with definite transformation properties, and the flavor content $\bar{q}Q$ is suppressed) can be measured by the symmetry breaking parameter

$$\kappa_{AB}(zT) = \frac{|C_A(zT) - C_B(zT)|}{C_A(zT) + C_B(zT)}, \quad z > 0. \tag{4}$$

If C_A and C_B are exactly degenerate at T, then $\kappa_{AB} = 0$ for any z, and the symmetry is effectively restored at T. On the other hand, if there is any discrepancy between C_A and C_B at any z, then κ_{AB} is nonzero at this z, and the symmetry is not exactly restored at T. Here the denominator of (4) serves as (re)normalization and the value of κ_{AB} is bounded between zero and one. Obviously, this criterion is more stringent than the equality of the screening masses, $m_A^{scr} = m_B^{scr}$, which are extracted from C_A and C_B at large z.

Note that κ_{AB} in (4) can be written as

$$\kappa_{AB}(zT) = \frac{|1 - C_B(zT)/C_A(zT)|}{1 + C_B(zT)/C_A(zT)},$$

which is different from the $\kappa_{AB}(zT) = |1 - C_B(zT)/C_A(zT)|$ used in Ref. [1]. Also, all z-correlators in (4), as well as those shown in Figs. 1-7 are *unnormalized*, while those in Ref. [1] are *normalized* by their values at $z/a = 1$ (i.e., $C_\Gamma(zT) = 1$ at $z/a = 1$). The former avoids any "accidental" degeneracies due to the normalization. In the following, any symmetry breaking parameter to measure the degeneracy of two meson z-correlators is always defined according to (4).

A. $SU(2)_L \times SU(2)_R$ and $U(1)$ symmetry breaking parameters

According to (4), the $SU(2)_L \times SU(2)_R$ symmetry breaking parameter can be written as

$$\kappa_{VA}(zT) = \frac{|C_{V_K}(zT) - C_{A_k}(zT)|}{C_{V_k}(zT) + C_{A_k}(zT)}, \quad z > 0, \quad (k = 1, 2, 4). \tag{5}$$

Due to the S_2 symmetry of the z-correlators, it only needs to examine $k = 1$ and $k = 4$ components of (5). In general, the difference between $k = 1$ and $k = 4$ components of (5) is negligible, thus in the following, we only give the results of (5) with $k = 1$.

In general, to determine to what extent the $SU(2)_L \times SU(2)_R$ chiral symmetry is manifested in the z-correlators, it is necessary to examine whether κ_{VA} is sufficiently small. To this end,

we use the following criterion for the manifestation of $SU(2)_L \times SU(2)_R$ chiral symmetry at T for a fixed zT

$$\kappa_{VA}(zT) \leq \epsilon_{VA}, \tag{6}$$

where ϵ_{VA} is a small parameter which defines the precision of the chiral symmetry. For fixed zT and ϵ_{VA}, the temperature T_c for the manifestation of the $SU(2)_L \times SU(2)_R$ symmetry is the lowest temperature satisfying (6), i.e.,

$$\kappa_{VA}(zT) < \epsilon_{VA} \text{ for } T > T_c. \tag{7}$$

In this study, we set ϵ_{VA} to two different values, 0.05 and 0.01, to study how T_c depends on ϵ_{VA}.

For the $U(1)_A$ symmetry breaking, it can be measured by the z-correlators in the pseudoscalar and scalar channels, with

$$\kappa_{PS}(zT) = \frac{|C_P(zT) - C_S(zT)|}{C_P(zT) + C_S(zT)}, \quad z > 0, \tag{8}$$

as well as in the tensor vector and axial-tensor vector channels, with

$$\kappa_{TX}(zT) = \frac{|C_{T_k}(zT) - C_{X_k}(zT)|}{C_{T_k}(zT) + C_{X_k}(zT)}, \quad z > 0, \quad (k = 1, 2, 4). \tag{9}$$

Due to the S_2 symmetry of the z-correlators, it only needs to examine $k = 1$ and $k = 4$ components of (9). In practice, the difference between $k = 1$ and $k = 4$ components of (9) is almost zero, up to the statistical uncertainties, thus in the following, we only give the results of (9) with $k = 4$.

In general, $\kappa_{PS}(zT) \neq \kappa_{TX}(zT)$. For consistency, we always use $\kappa_{TX}(zT)$ (9) with $k = 4$ to measure the $U(1)_A$ symmetry breaking.

Similar to (6), we use the following criterion for the manifestation of $U(1)_A$ symmetry at T for a fixed zT

$$\kappa_{TX}(zT) \leq \epsilon_{TX}, \tag{10}$$

where ϵ_{TX} is a small parameter which defines the precision of $U(1)_A$ symmetry. For fixed zT and ϵ_{TX}, the temperature T_1 for the manifestation of $U(1)_A$ symmetry is the lowest temperature satisfying (10), i.e.,

$$\kappa_{TX}(zT) < \epsilon_{TX} \text{ for } T > T_1. \tag{11}$$

In this study, we set ϵ_{TX} to two different values, 0.05 and 0.01, to study how the temperature of restoration of $U(1)_A$ symmetry depends on ϵ_{TX}.

Next, consider QCD with $N_f = 2 + 1(+1)(+1)$ quarks $(q_1, q_2, \cdots, q_{N_f})$. As discussed in Sec. I, upon neglecting the disconnected diagrams in the meson z-correlators, the $SU(N)_L \times SU(N)_R$ chiral symmetry of N $(2 \leq N \leq N_f)$ quarks is manifested by the degeneracies of meson z-correlators in the vector and axial-vector channels, $C_{V_k}^{\bar{q}_i q_j}(z) = C_{A_k}^{\bar{q}_i q_j}(z)$, $(k = 1, 2, 4)$, for *all* flavor combinations of N quarks $(\bar{q}_i q_j, \; i, j = 1, \cdots, N)$. Thus, to determine the temperature T_c for the manifestation of the $SU(N)_L \times SU(N)_R$ chiral symmetry of N quarks, it needs to measure $\kappa_{VA}^{\bar{q}_i q_j}$ for *all* flavor combinations of N quarks, and check whether they *all* satisfy the criterion (6) for fixed zT and ϵ_{VA}. This amounts to finding the largest $T_c^{\bar{q}_i q_j}$ satisfying (6) among all flavor combinations of N quarks, i.e.,

$$T_c = \max(T_c^{\bar{q}_i q_j}, i, j = 1, 2, \cdots, N). \tag{12}$$

About the $U(1)_A$ chiral symmetry of N $(2 \leq N \leq N_f)$ quarks, upon neglecting the disconnected diagrams in the meson z-correlators, it is manifested by the degeneracies of meson z-correlators in the pseudoscalar and scalar channels, $C_P^{\bar{q}_i q_j}(z) = C_S^{\bar{q}_i q_j}(z)$, as well as in the tensor vector and axial-tensor vector channels, $C_{T_k}^{\bar{q}_i q_j}(z) = C_{X_k}^{\bar{q}_i q_j}(z)$, $(k = 1, 2, 4)$, for *all* flavor combinations of N quarks $(\bar{q}_i q_j, \; i, j = 1, \cdots, N)$. Thus, to determine the temperature T_1 for the manifestation of the $U(1)_A$ symmetry via the $k = 4$ component of the tensor vector and axial-tensor vector channels, it needs to measure $\kappa_{TX}^{\bar{q}_i q_j}$ for *all* flavor combinations of N quarks, and check whether they *all* satisfy the criterion (10) for fixed zT and ϵ_{TX}. This amounts to finding the largest $T_1^{\bar{q}_i q_j}$ satisfying (10) among all flavor combinations of N quarks, i.e.,

$$T_1 = \max(T_1^{\bar{q}_i q_j}, i, j = 1, 2, \cdots, N). \tag{13}$$

B. $SU(2)_{CS}$ symmetry breaking and fading parameters

Following the discussion and notations in Ref. [1], the $SU(2)_{CS}$ multiplets for the z-correlators with flavor content $\bar{q}Q$ are

$$(V_1); \; (A_1, T_4, X_4), \tag{14}$$

$$(V_4); \; (A_4, T_1, X_1), \tag{15}$$

where the "2" components due to the S_2 symmetry have been suppressed. Thus the degeneracies in the above triplets signal the emergence of $SU(2)_{CS}$ chiral spin symmetry. For $T \geq T_{c1}^{\bar{q}Q}$, the $SU(2)_L \times SU(2)_R \times U(1)_A$ chiral symmetry is effectively restored, and $C_{V_k} = C_{A_k}$ and $C_{T_k} = C_{X_k}$ for $k = 1, 2, 4$, and the multiplets in Eqs. (14) and (15) become:

$$(V_1, A_1, T_4, X_4), \tag{16}$$

$$(V_4, A_4, T_1, X_1). \tag{17}$$

This suggests the possibility of a larger symmetry group $SU(4)$ for $T > T_{c1}^{\bar{q}Q}$ which contains $SU(2)_L \times SU(2)_R \times SU(2)_{CS}$ as a subgroup. For the full $SU(4)$ symmetry, each of the multiplets in Eqs. (16) and (17) is enlarged to include the flavor-singlet partners of A_k, T_k and X_k, while the flavor-singlet partners of V_1 and V_4 are $SU(4)$ singlets, i.e.,

$$V_1^0; \ (V_1, A_1, T_4, X_4, A_1^0, T_4^0, X_4^0), \tag{18}$$

$$V_4^0; \ (V_4, A_4, T_1, X_1, A_4^0, T_1^0, X_1^0), \tag{19}$$

where the superscript "0" denotes the flavor singlet.

In general, to examine the emergence of $SU(2)_{CS}$ symmetry, one needs to measure the splittings in both (A_1, X_4) and (T_4, X_4) of (14). To measure the splitting of A_1 and X_4, we use

$$\kappa_{AT}(zT) = \frac{|C_{A_1}(zT) - C_{X_4}(zT)|}{C_{A_1}(zT) + C_{X_4}(zT)}, \quad z > 0, \tag{20}$$

while the splitting of T_4 and X_4 is measured by κ_{TX} (9) with $k = 4$. Then we use the maximum of κ_{AT} and κ_{TX} to measure the $SU(2)_{CS}$ symmetry breaking, with the parameter

$$\kappa_{CS} = \max(\kappa_{AT}, \kappa_{TX}). \tag{21}$$

Note that for $(\bar{u}d, \bar{u}s, \bar{s}s, \bar{u}c)$ sectors, $\kappa_{AT}(zT) > \kappa_{TX}(zT)$ for all z and the seven temperatures in this study, thus $\kappa_{CS} = \kappa_{AT}$.

As the temperature T is increased, the separation between the multiplets of $SU(2)_{CS}$ and $U(1)_A$ is decreased. Therefore, at sufficiently high temperatures, the $U(1)_A$ multiplet $M_0 = (P, S)$ and the $SU(2)_{CS} \times SU(2)_L \times SU(2)_R$ multiplet $M_2 = (V_1, A_1, T_4, X_4)$ merge together, then the approximate $SU(2)_{CS}$ symmetry becomes washed out, and only the $SU(2)_L \times SU(2)_R \times U(1)_A$ chiral symmetry remains. Note that the $SU(2)_{CS} \times SU(2)_L \times SU(2)_R$

multiplet $M_4 = (V_4, A_4, T_1, X_1)$ never merges with M_0 and M_2 even in the limit $T \to \infty$, as discussed in Ref. [1]. Thus M_4 is irrelevant to the fading of the approximate $SU(2)_{CS}$ symmetry.

Here we use the $SU(2)_{CS}$ symmetry fading parameter similar to that defined in Ref. [1], except for taking the absolute value and using the unnormalized z-correlators, i.e.,

$$\kappa(zT) = \left| \frac{C_{A_1}(zT) - C_{X_4}(zT)}{C_{M_0}(zT) - C_{M_2}(zT)} \right|, \quad z > 0, \tag{22}$$

where

$$C_{M_0}(zT) \equiv \frac{1}{2} \left[C_P(zT) + C_S(zT) \right],$$

$$C_{M_2}(zT) \equiv \frac{1}{4} \left[C_{V_1}(zT) + C_{A_1}(zT) + C_{T_4}(zT) + C_{X_4}(zT) \right].$$

In general, $\kappa(zT)$ behaves like an increasing function of T for a fixed zT. If $\kappa(zT) \ll 1$ for a range of T, then the approximate $SU(2)_{CS}$ symmetry is well-defined for this window of T. On the other hand, if $\kappa(zT) > 0.3$ for $T > T_f$, then the approximate $SU(2)_{CS}$ symmetry is regarded to be washed out, and only the $U(1)_A \times SU(2)_L \times SU(2)_R$ chiral symmetry remains. Thus, to determine to what extent the $SU(2)_{CS}$ symmetry is manifested in the z-correlators, it is necessary to examine whether both $\kappa(zT)$ and $\kappa_{CS}(zT)$ are sufficiently small. For a fixed zT, the following condition

$$(\kappa_{CS}(zT) < \epsilon_{cs}) \ \wedge \ (\kappa(zT) < \epsilon_{fcs}) \tag{23}$$

serves as a criterion for the approximate $SU(2)_{CS}$ symmetry in the z-correlators, where ϵ_{cs} is for the $SU(2)_{CS}$ symmetry breaking, while ϵ_{fcs} for the $SU(2)_{CS}$ symmetry fading. For fixed zT, (23) gives a window of T for the approximate $SU(2)_{CS}$ symmetry. Obviously, the size of this window depends on ϵ_{cs} and ϵ_{fcs}. That is, larger ϵ_{cs} or ϵ_{fcs} gives a wider window of T, and conversely, smaller ϵ_{cs} or ϵ_{fcs} gives a narrower window of T.

IV. Meson z-correlators of $(\bar{u}d, \bar{u}s, \bar{s}s, \bar{u}c, \bar{s}c, \bar{c}c)$

Following the prescription proposed in Ref. [1] for the cancellation of the contribution of unphysical meson states to the z-correlators, we compute two sets of quark propagators with periodic and antiperiodic boundary conditions in the z direction, while their boundary

FIG. 1.   The spatial z-correlators of meson interplotors for six flavor combinations ($\bar{u}d$, $\bar{u}s$, $\bar{s}s$, $\bar{u}c$, $\bar{s}c$, and $\bar{c}c$) in $N_f = 2+1+1$ lattice QCD at $T \simeq 192$ MeV.
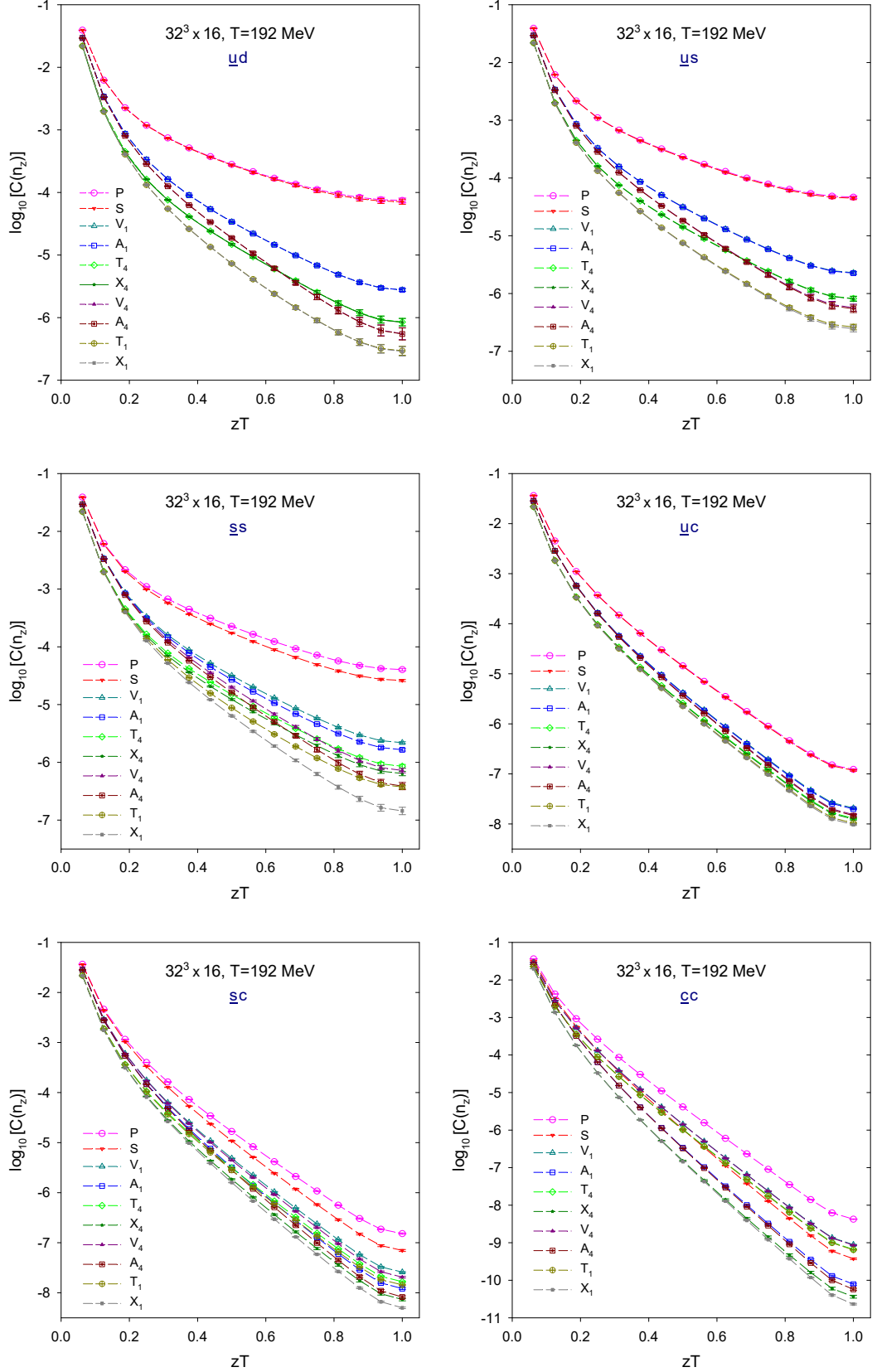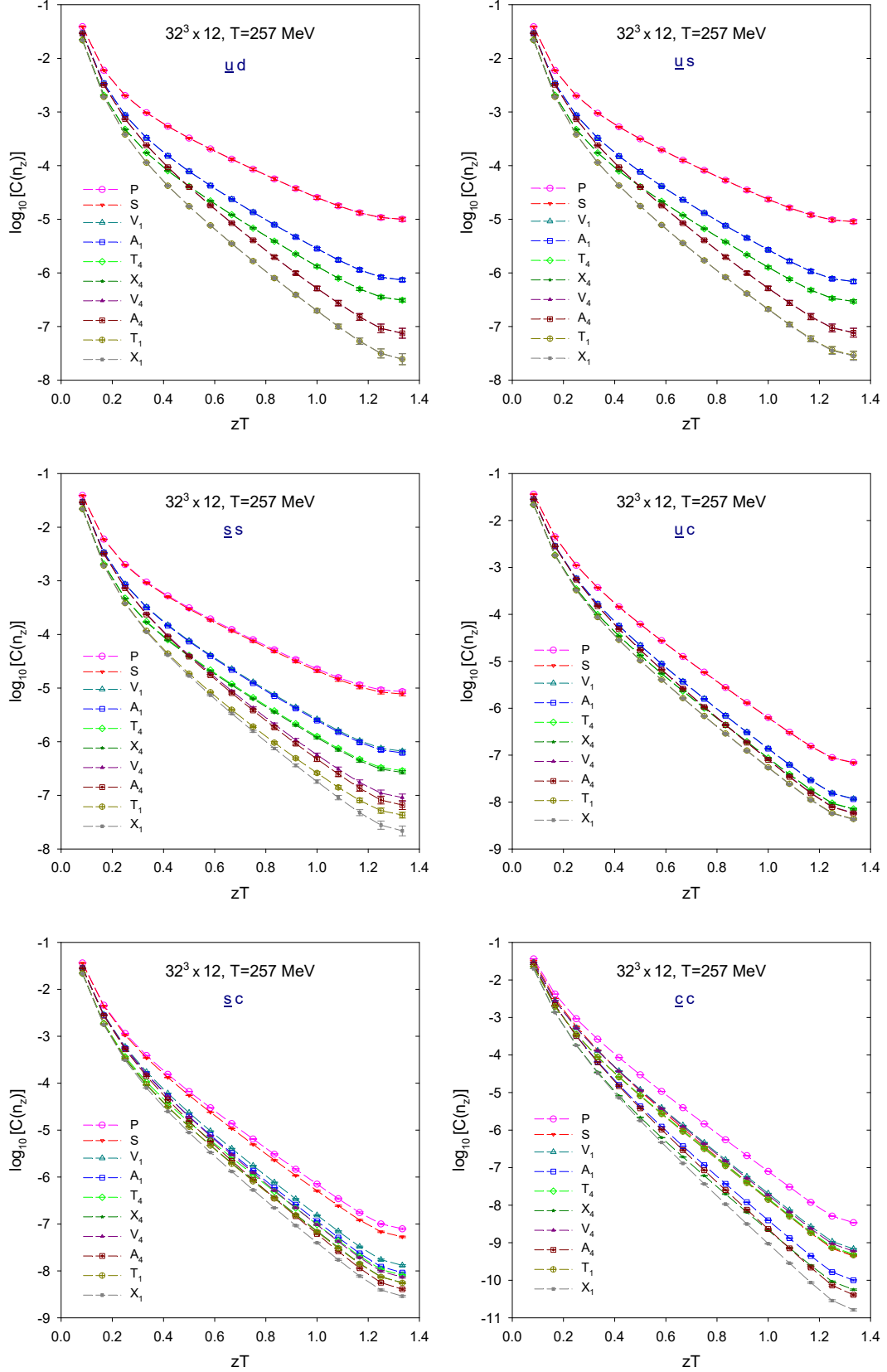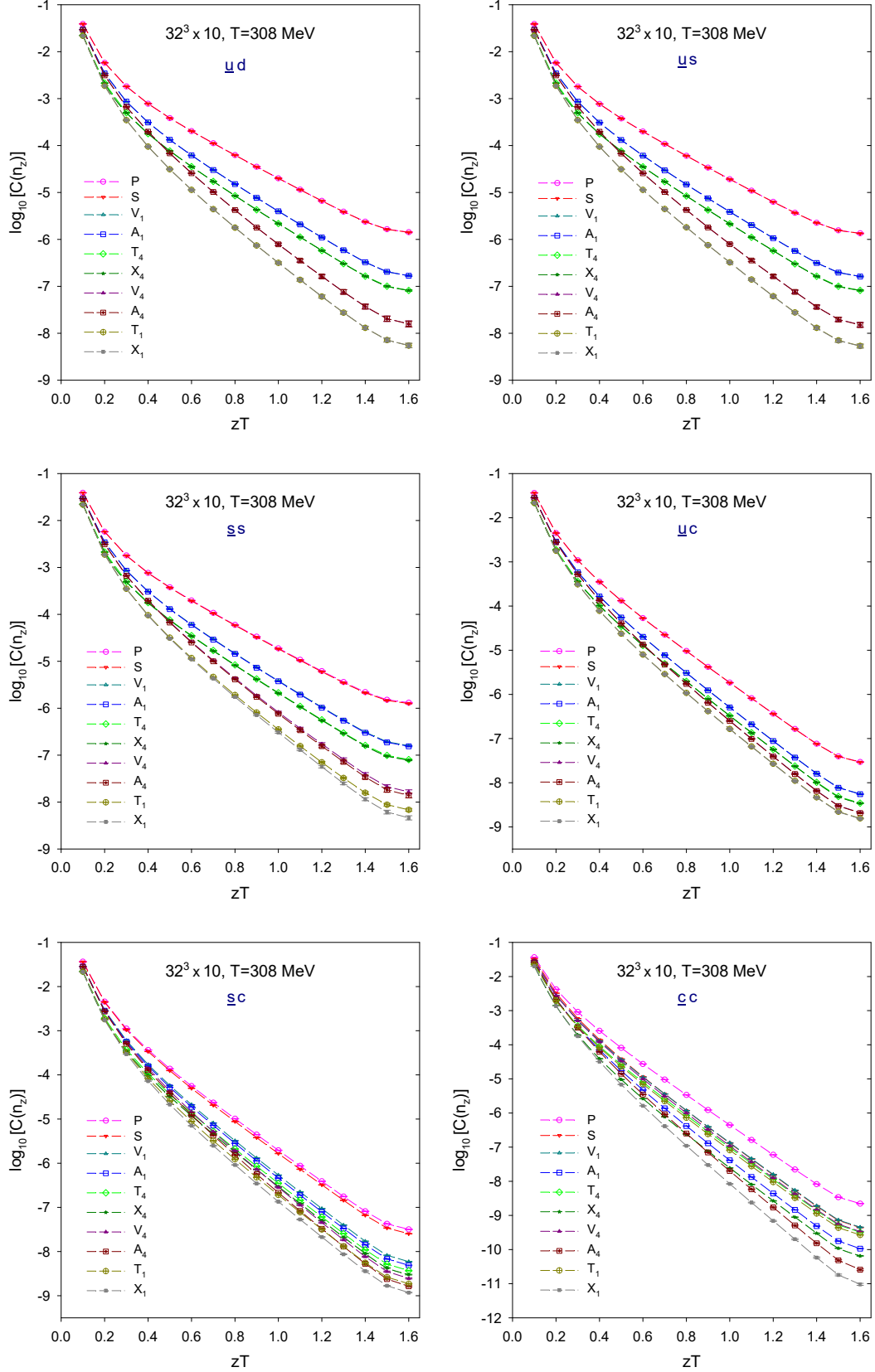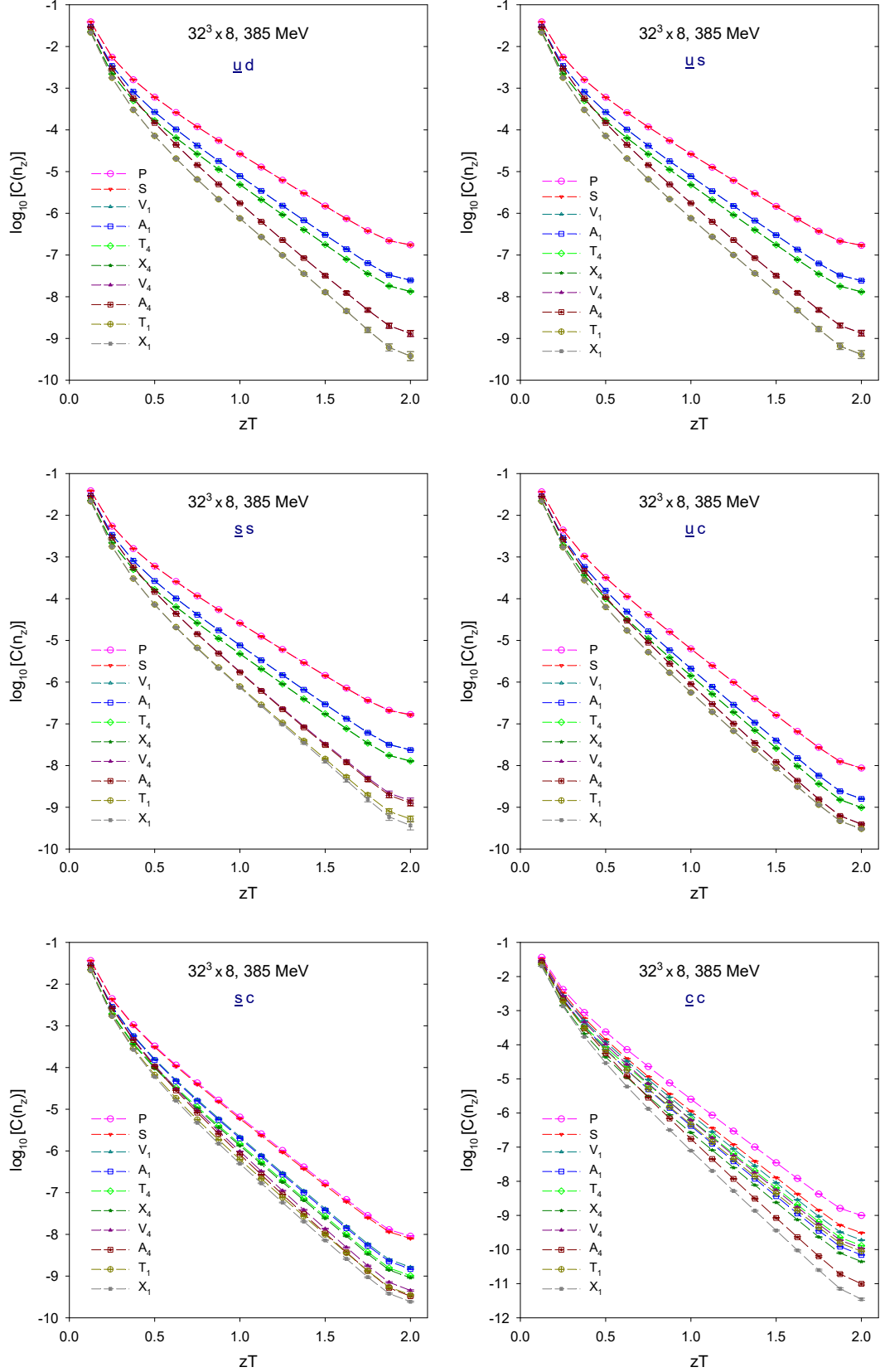
FIG. 2.   The spatial z-correlators of meson interplotors for six flavor combinations ($\bar{u}d$, $\bar{u}s$, $\bar{s}s$, $\bar{u}c$, $\bar{s}c$, and $\bar{c}c$) in $N_f = 2 + 1 + 1$ lattice QCD at $T \simeq 257$ MeV.

FIG. 3. The spatial z-correlators of meson interplotors for six flavor combinations ($\bar{u}d$, $\bar{u}s$, $\bar{s}s$, $\bar{u}c$, $\bar{s}c$, and $\bar{c}c$) in $N_f = 2 + 1 + 1$ lattice QCD at $T \simeq 308$ MeV.
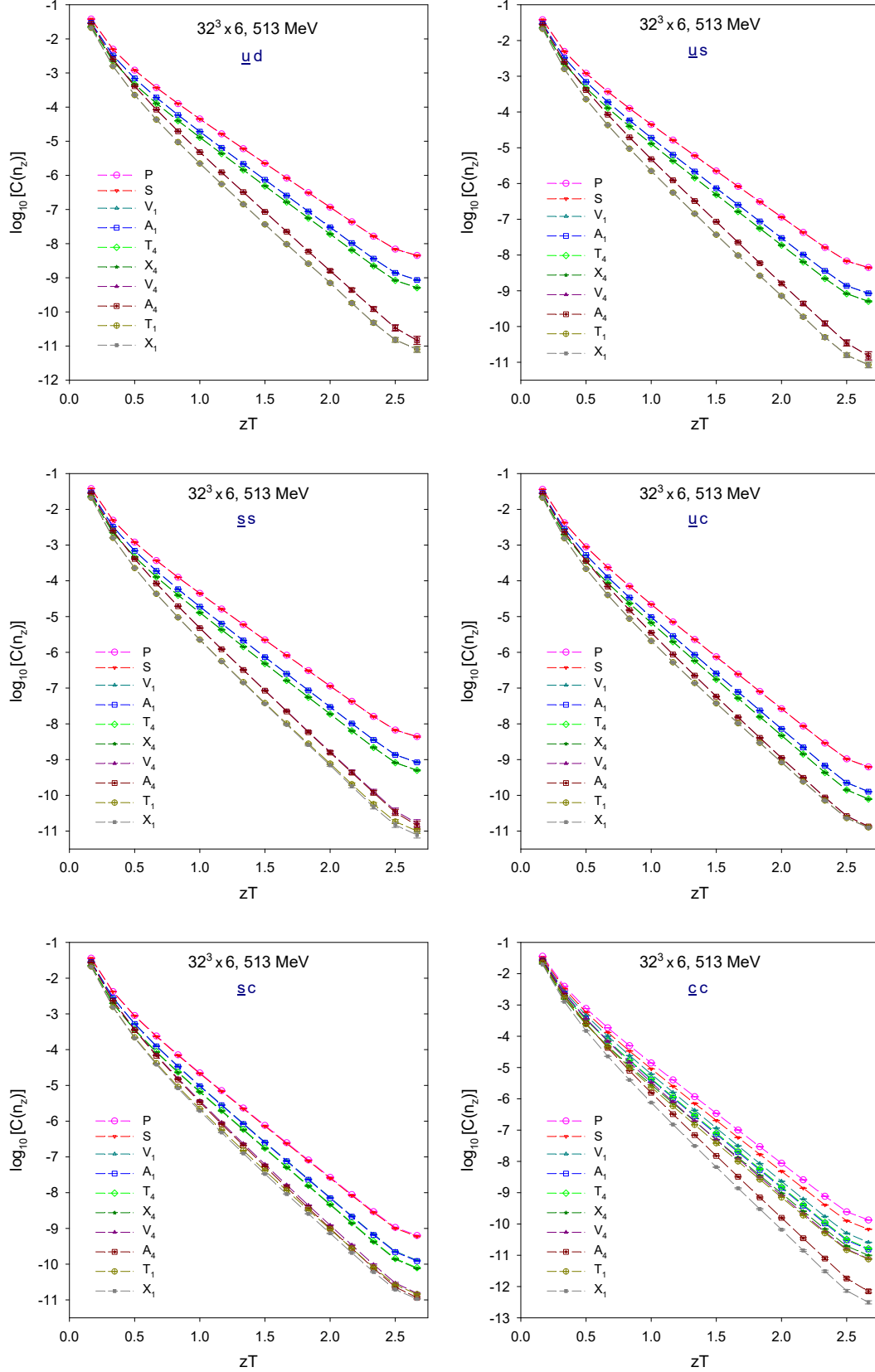
FIG. 4.   The spatial z-correlators of meson interplotors for six flavor combinations ($\bar{u}d$, $\bar{u}s$, $\bar{s}s$, $\bar{u}c$, $\bar{s}c$, and $\bar{c}c$) in $N_f = 2 + 1 + 1$ lattice QCD at $T \simeq 385$ MeV.
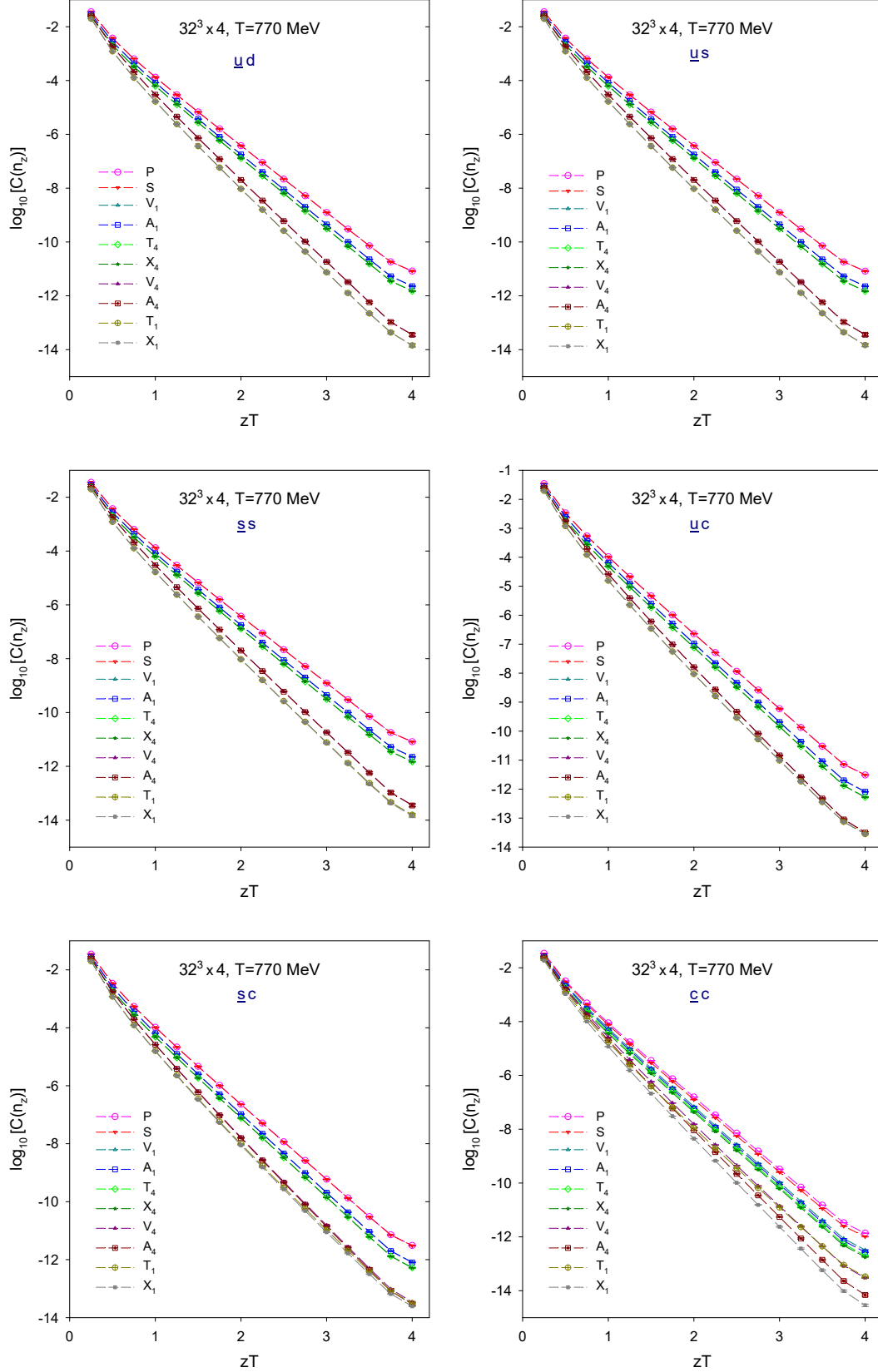
FIG. 5. The spatial z-correlators of meson interplotors for six flavor combinations ($\bar{u}d$, $\bar{u}s$, $\bar{s}s$, $\bar{u}c$, $\bar{s}c$, and $\bar{c}c$) in $N_f = 2+1+1$ lattice QCD at $T \simeq 513$ MeV.

FIG. 6. The spatial z-correlators of meson interplotors for six flavor combinations ($\bar{u}d$, $\bar{u}s$, $\bar{s}s$, $\bar{u}c$, $\bar{s}c$, and $\bar{c}c$) in $N_f = 2 + 1 + 1$ lattice QCD at $T \simeq 770$ MeV.
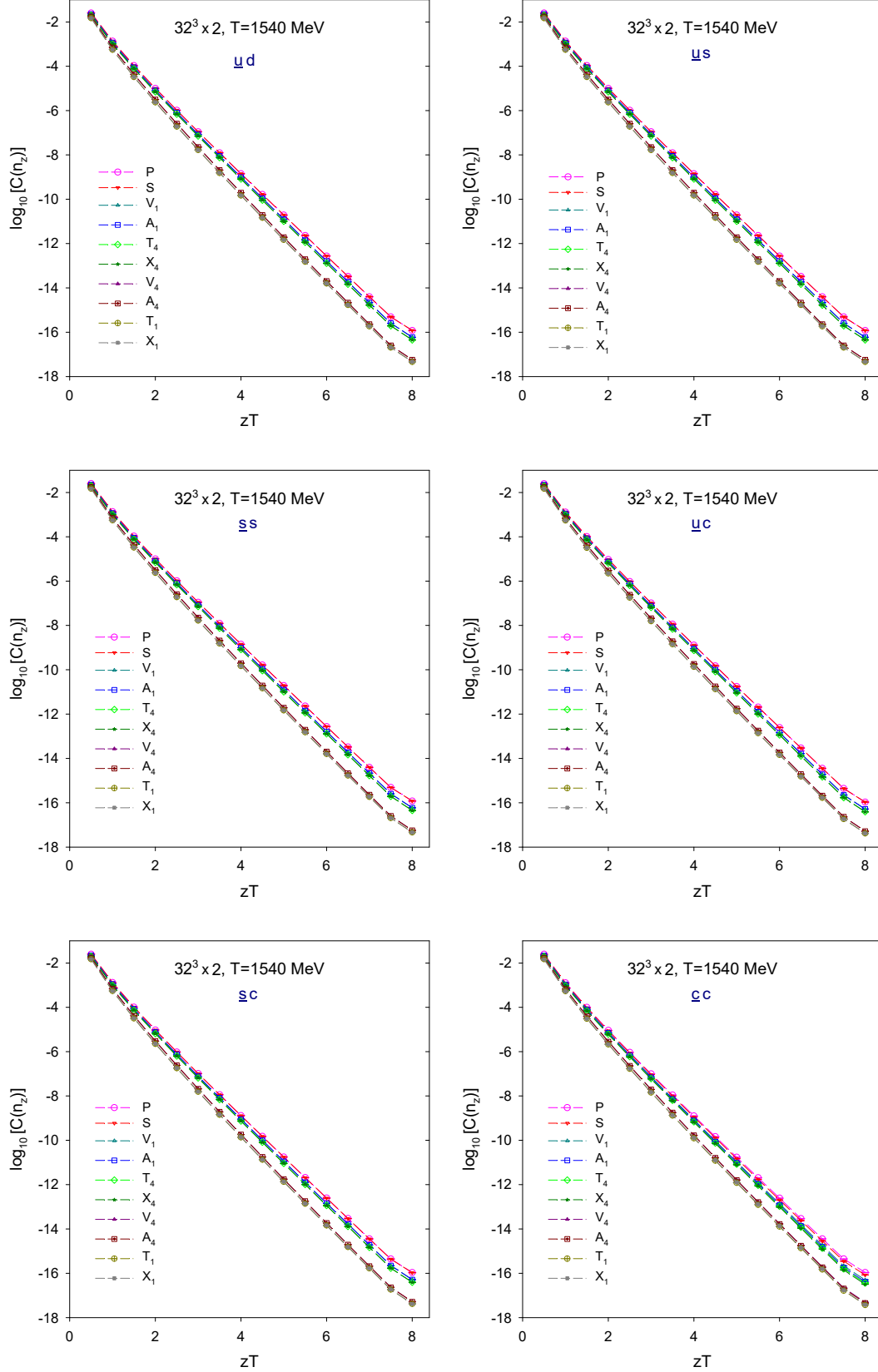
FIG. 7. The spatial z-correlators of meson interplotors for six flavor combinations ($\bar{u}d$, $\bar{u}s$, $\bar{s}s$, $\bar{u}c$, $\bar{s}c$, and $\bar{c}c$) in $N_f = 2+1+1$ lattice QCD at $T \simeq 1540$ MeV.

conditions in (x, y, t) directions are the same, i.e., periodic in the (x, y) directions, and antiperiodic in the t direction. Each set of quark propagators are used to construct the z correlators independently, and finally taking the average of these two z correlators. Then, the contribution of unphysical meson states to the z correlators can be cancelled configuration by configuration, up to the numerical precision of the quark propagators.

In each of Figs. 1-7, the z-correlators for six flavor contents $(\bar{u}d, \bar{u}s, \bar{s}s, \bar{u}c, \bar{s}c, \bar{c}c)$ at the same T are plotted as a function of the dimensionless variable zT (3). Due to the degeneracy (the S_2 symmetry) of the "1" and "2" components in the z correlators of vector mesons, only the "1" components are plotted. In general, each panel plots ten $C_\Gamma(zT)$ for $\Gamma = \{P, S, V_1, A_1, T_4, X_4, V_4, A_4, T_1, X_1\}$. For the classification and notations of meson interpolators, see Table II.

TABLE II. The classification of meson interpolators $\bar{q}_1 \Gamma q_2$, and their names and notations.

Name and notation	Γ (for z correlators)
Scalar (S)	$\mathbb{1}$
Pseudocalar (P)	γ_5
Vector (V_k)	$\gamma_k \ (k = 1, 2, 4)$
Axial vector (A_k)	$\gamma_5 \gamma_k \ (k = 1, 2, 4)$
Tensor vector (T_k)	$\gamma_3 \gamma_k \ (k = 1, 2, 4)$
Axial-tensor vector (X_k)	$\gamma_5 \gamma_3 \gamma_k \ (k = 1, 2, 4)$

For any flavor combination, if the $SU(2)_L \times SU(2)_R$ chiral symmetry is restored, then its (V_1, A_1) and (V_4, A_4) become degenerate, and the number of distinct z-correlators appears to be reduced to eight. Furthermore, if the $U(1)_A$ symmetry is also restored, then its (P, S), (T_4, X_4) and (T_1, X_1) also become degenerate, and the number of distinct z-correlators is further reduced to five. Thus one can visualize the effective retoration of $SU(2)_L \times SU(2)_R \times U(1)_A$ chiral symmetry when the number of distinct z-correctors becomes five. This provides a simple guideline to look for the restoration of chiral symmetry from the panels in Figs. 1-7.

Following the above guidline, we can visually identify the hierarchical rstoration of chiral symmetries in $N_f = 2 + 1 + 1$ QCD with (u, d, s, c) quarks.

In Fig. 1, at $T = 192$ MeV, we see that both $T_c^{\bar{u}d}$ (the temperature for the restoration of $SU(2)_L \times SU(2)_R$ chiral symmetry in the $\bar{u}d$ sector) and T_1^{ud} (the temperature for the restoration of $U(1)_A$ symmetry in the $\bar{u}d$ sector) are lower than 190 MeV, i.e., $T_c^{\bar{u}d} < 190$ MeV and $T_1^{\bar{u}d} < 190$ MeV. Thus the $SU(2)_L \times SU(2)_R \times U(1)_A$ chiral symmetry of $\bar{u}d$ has been restored at some temperature lower than 190 MeV, i.e., $T_{c1}^{\bar{u}d} < 190$ MeV.

Moreover, in Fig. 1, the panels of $\bar{u}s$ and $\bar{u}c$ show that $T_c^{\bar{u}s} < 190$ MeV, $T_1^{\bar{u}s} < 190$ MeV, $T_c^{\bar{u}c} < 190$ MeV, and $T_1^{\bar{u}c} < 190$ MeV. Thus, $T_{c1}^{\bar{u}s} < 190$ MeV, and $T_{c1}^{\bar{u}c} < 190$ MeV,

Next we look at the $\bar{s}s$ panels in Figs. 1-7. In Fig. 2, at $T = 257$ MeV, it appears to have five distinct z-correlators in the channels of (P, S), (V_1, A_1), (T_4, X_4), (V_4, A_4) and (T_1, X_1), in spite of the small splittings at large z in the channels of (V_4, A_4) and (T_1, X_1). Thus the $SU(2)_L \times SU(2)_R \times U(1)_A$ chiral symmetry of $\bar{s}s$ can be regarded to be restored at $T_{c1}^{\bar{s}s} \sim 257$ MeV. This implies that the $SU(3)_L \times SU(3)_R \times U(1)_A$ chiral symmetry of (u, d, s) quarks is restored at $T_{c1}^{\bar{s}s} \sim 257$ MeV, since the the $SU(2)_L \times SU(2)_R \times U(1)_A$ chiral symmetry in both $\bar{u}d$ and $\bar{u}s$ sectors has been restored at $T < 190$ MeV. This is the first step of the hierarchical restoration of chiral symmetries in $N_f = 2+1+1$ lattice QCD at the physical point, from the restoration of $SU(2)_L \times SU(2)_R \times U(1)_A$ chiral symmetry of (u, d) quarks at $T_{c1}^{\bar{u}d} < 190$ MeV to the restoratrion of $SU(3)_L \times SU(3)_R \times U(1)_A$ chiral symmetry of (u, d, s) quarks at $T_{c1}^{\bar{s}s} \sim 257$ MeV.

Note that, as discussed in Sec. I and Sec. III, the restoration of $SU(3)_L \times SU(3)_R \times U(1)_A$ chiral symmetry of (u, d, s) quarks requires the $SU(2)_L \times SU(2)_R \times U(1)_A$ chiral symmetry for all six flavor combinations ($\bar{u}d$, $\bar{u}s$, $\bar{d}s$, $\bar{u}u$, $\bar{d}d$, $\bar{s}s$), which are reduced to ($\bar{u}d$, $\bar{u}s$, $\bar{s}s$) if $m_u = m_d$. Here we have assumed that in high temperature QCD, the contribution of the disconnected diagrams to the z-correlator of $\bar{q}\Gamma q$ is negligible in comparison with that of the connected ones, as discussed in Sec. I. Similarly, the restoration of $SU(4)_L \times SU(4)_R \times U(1)_A$ chiral symmetry of $(u/d, d, s, c)$ quarks requires the $SU(2)_L \times SU(2)_R \times U(1)_A$ chiral symmetry for all six flavor combinations $\bar{u}d$, $\bar{u}s$, $\bar{s}s$, $\bar{u}c$, $\bar{s}c$, and $\bar{c}c$.

Next, we look at the $\bar{s}c$ panels in Figs. 1-7. The $SU(2)_L \times SU(2)_R \times U(1)_A$ chiral symmetry seems to manifest at $T = 385$ MeV, and it becomes highly pronounced at $T = 513$ MeV. This implies that $T_{c1}^{\bar{s}c}$ is in the range of 385-512 MeV. In general, a more precise estimate of T_c and T_1 can be obtained by the criteria (6) and (10), which will be given in the next

section.

Finally, we look at the $\bar{c}c$ panels in Figs. 1-7. The $SU(2)_L \times SU(2)_R \times U(1)_A$ chiral symmetry of $\bar{c}c$ seems to manifest at $T = 770$ MeV, and it becomes highly pronounced at $T = 1540$ MeV. This implies that $T_{c1}^{\bar{c}c}$ is in the range of 770-1540 MeV, and also the restoratrion of the $SU(4)_L \times SU(4)_R \times U(1)_A$ chiral symmetry of (u, d, s, c) quarks at $T_{c1}^{\bar{c}c} \sim$ 770-1540 MeV, since the $SU(2)_L \times SU(2)_R \times U(1)_A$ chiral symmetry in other sectors $(\bar{u}d, \bar{u}s, \bar{s}s, \bar{u}c, \bar{s}c)$ has already been restored at lower temperatures. This gives the second step of the hierarchical restoration of chiral symmetries in $N_f = 2 + 1 + 1$ lattice QCD at the physical point, from the restoration of the $SU(3)_L \times SU(3)_R \times U(1)_A$ chiral symmetry of (u, d, s) quarks at $T_{c1}^{\bar{s}s} \sim 257$ MeV to the restoratrion of $SU(4)_L \times SU(4)_R \times U(1)_A$ chiral symmetry of (u, d, s, c) quarks at $T_{c1}^{\bar{c}c} \sim 770 - 1540$ MeV. A more precise estimate of $T_c^{\bar{c}c}$ and T_1^{barcc} can be obtained by the criteria (6) and (10), which will be given in the next subsection.

Besides the hierarchical restoration of chiral symmetries, we are also interested in visually identifying the emergence of the approximate $SU(2)_{CS}$ chiral spin symmetry in each of the six flavor sectors. To this end, we look for the appearance of three approximately distinct multiplets

$$M_0 = (P, S),$$
$$M_2 = (V_1, A_1, T_4, X_4),$$
$$M_4 = (V_4, A_4, T_1, X_1),$$

which become more pronounced at higher temperatures, and they are in the order

$$C_{M_0} > C_{M_2} > C_{M_4}.$$

The emergence of M_2 and M_4 is in agreement with the $SU(2)_{CS}$ multiplets of (14) and (15), and the $SU(2)_{CS} \times SU(2)_L \times SU(2)_R$ multiplets of (16) and (17). This suggests the emergence of the approximate $SU(2)_{CS}$ and $SU(4)$ symmetries. Moreover, the separation between the multiplets M_2 and M_0 is decreased as the temperature is increased further. Thus, at sufficiently high temperatures, say $T > T_f$, M_2 and M_0 merges together to form a single multiplet, then the approximate $SU(2)_{CS}$ symmetry becomes washed out, and only the $SU(2)_L \times SU(2)_R \times U(1)_A$ chiral symmetry remains. In other words, the approximate $SU(2)_{CS}$ symmetry can only appear in a window of T above T_{c1}, i.e., $T_{c1} < T_{cs} \lesssim T \lesssim T_f$,

where T_{cs} (T_f) depends on ϵ_{cs} (ϵ_{fcs}) in the criterion (23) for the emergence (fading) of the approximate $SU(2)_{CS}$ symmetry. Note that the multiplet M_4 never merges with the multiplets M_0 and M_2, even in the limit $T \to \infty$, as discussed in Ref. [1]. Thus M_4 is irrelevant to the fading of the approximate $SU(2)_{CS}$ symmetry. The above provides a guideline to look for the emergence and the fading of the approximate $SU(2)_{CS}$ symmetry in Figs. 1-7.

First, we look at the panels of $\bar{u}d$ and $\bar{u}s$ in Figs. 1-7. We see that their z-correlators are almost identical for all seven temperatures. Furthermore, as T is increased from 192 MeV to 770 MeV, we see the emergence of three approximately distinct multiplets M_0, M_2, and M_4, which become more pronounced at higher temperatures, while the separation of M_0 and M_2 become smaller. This suggests the emergence of the approximate $SU(2)_{CS}$ and $SU(4)$ symmetries in the window $T \sim 308\text{-}770$ MeV, for both $\bar{u}d$ and $\bar{u}s$ sectors. Finally, at $T = 1540$ MeV, M_0 and M_2 (for any flavor combination) merge together to form a single multiplet, and the approximate $SU(2)_{CS}$ symmetry has become completely washed out, and only the chiral symmetry remains.

Next, from the $\bar{s}s$ panels in Figs. 1-7, we see that its window for the approximate $SU(2)_{CS}$ symmetry is almost the same as that of $\bar{u}d$ and $\bar{u}s$, i.e., $T \sim 308\text{-}770$ MeV.

Finally, we visually estimate the windows of the approximate $SU(2)_{CS}$ symmetry for heavy mesons with the c quark, which seem to be simlar to that of the light mesons. However, if one performs a more precise estimate with the criterion (23), one can reveal some salient features of the heavy vector mesons which cannot be easily observed by visual estimate, as shown in the next section.

V. Symmetry breaking parameters of $(\bar{u}d, \bar{u}s, \bar{s}s, \bar{u}c, \bar{s}c, \bar{c}c)$

In this section, we use the criteria (6), (10), and (23) to obtain T_c (the temperature for the restoration of $SU(2)_L \times SU(2)_R$ chiral symmetry), T_1 (the temperature for the restoration of $U(1)_A$ symmetry), and the window of T for the emergence of the approximate $SU(2)_{CS}$ symmetry, for six flavor combinations $(\bar{u}d, \bar{u}s, \bar{s}s, \bar{u}c, \bar{s}c, \bar{c}c)$ respectively. To this end, we use the z-correlators in Figs. 1-7 to compute the symmetry-breaking parameters κ_{VA}, κ_{PS}, κ_{TX},

FIG. 8.   The symmetry breaking parameters of spatial z-correlators of meson interplotors of six flavor combinations ($\bar{u}d$, $\bar{u}s$, $\bar{s}s$, $\bar{u}c$, $\bar{s}c$, and $\bar{c}c$) in $N_f = 2 + 1 + 1$ lattice QCD at $T \simeq 192$ MeV.
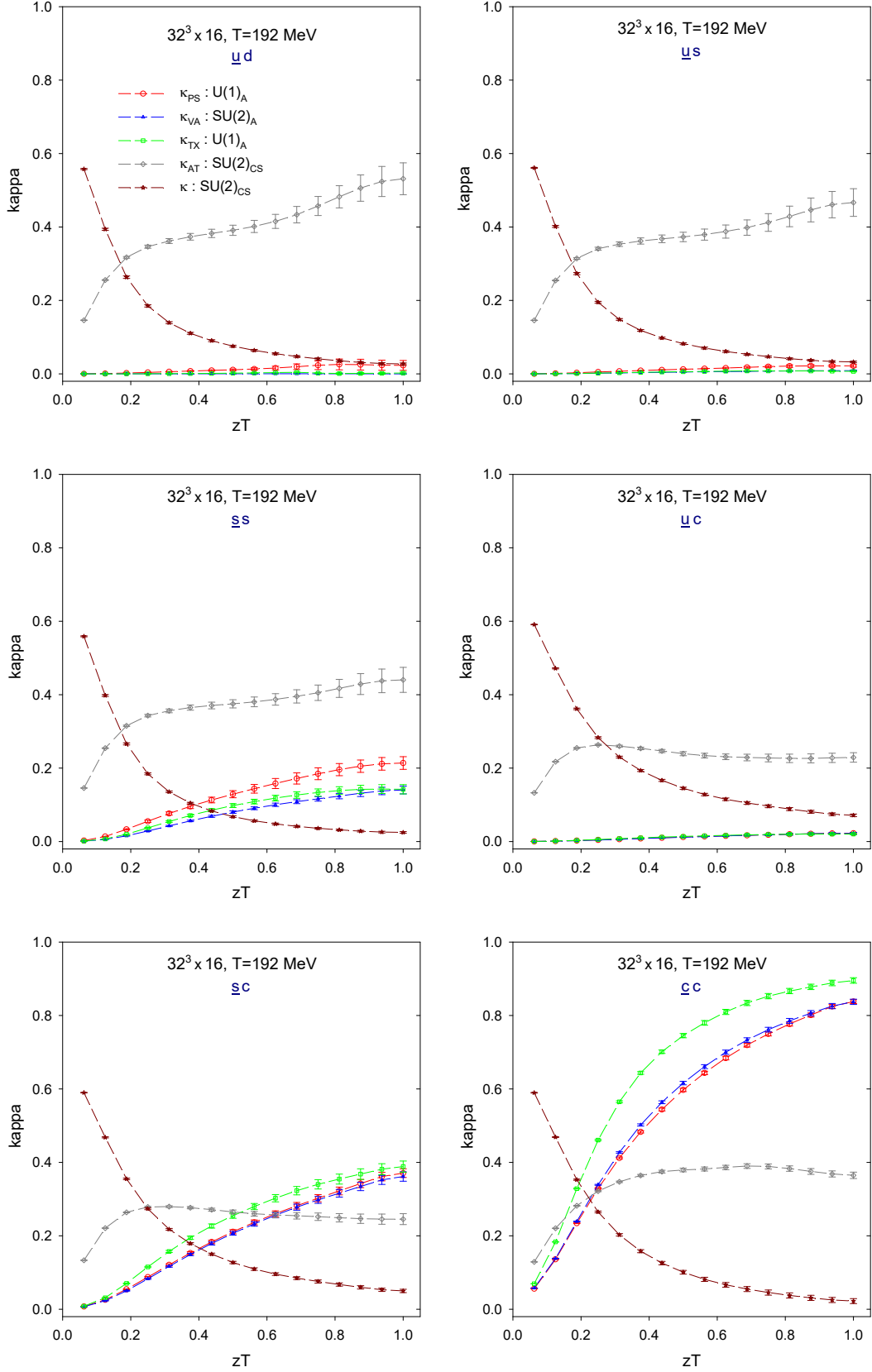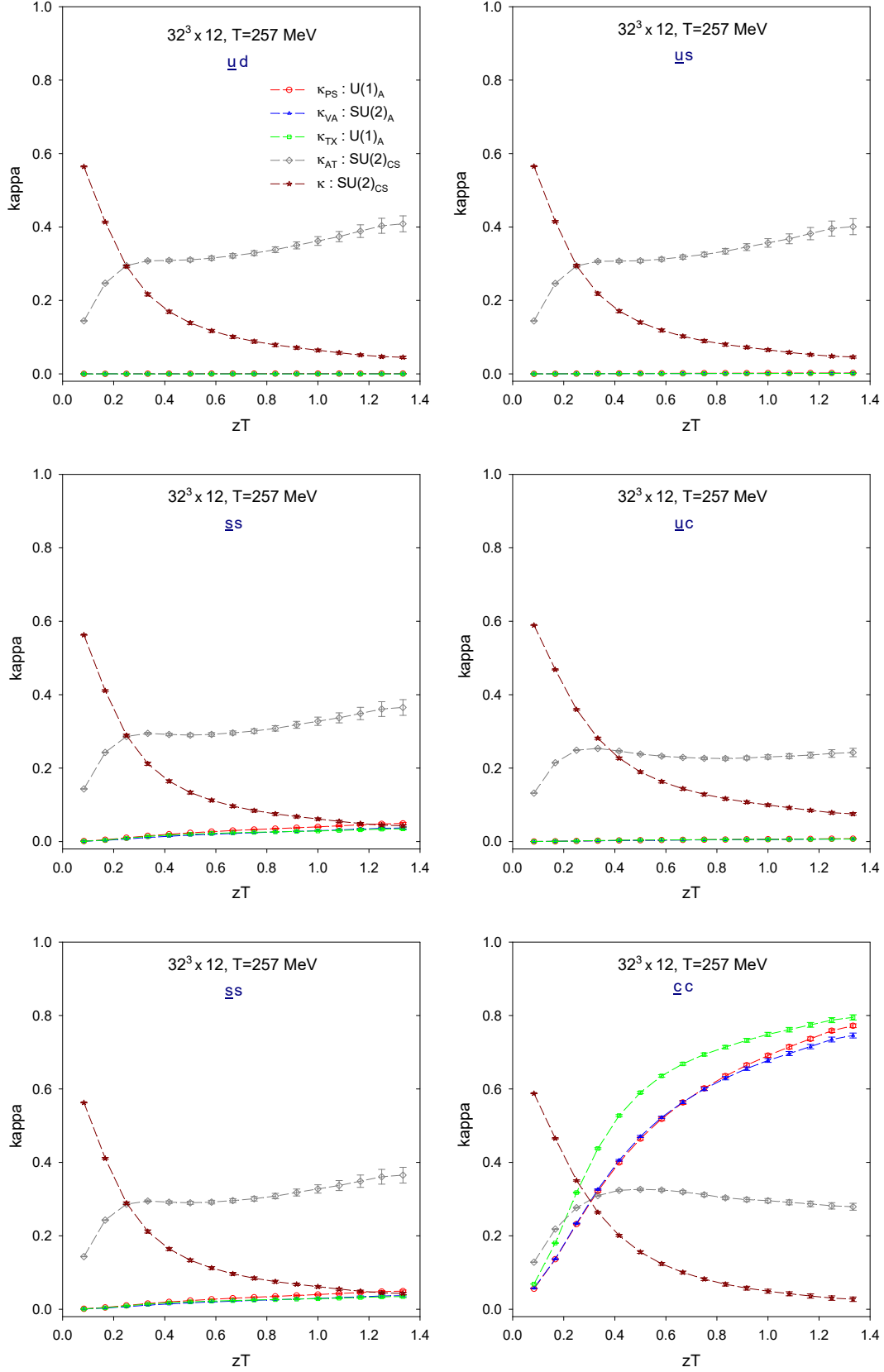
FIG. 9.   The symmetry breaking parameters of spatial z-correlators of meson interplotors of six flavor combinations ($\bar{u}d$, $\bar{u}s$, $\bar{s}s$, $\bar{u}c$, $\bar{s}c$, and $\bar{c}c$) in $N_f = 2 + 1 + 1$ lattice QCD at $T \simeq 257$ MeV.

FIG. 10. The symmetry breaking parameters of spatial z-correlators of meson interplotors of six flavor combinations ($\bar{u}d$, $\bar{u}s$, $\bar{s}s$, $\bar{u}c$, $\bar{s}c$, and $\bar{c}c$) in $N_f = 2 + 1 + 1$ lattice QCD at $T \simeq 308$ MeV.
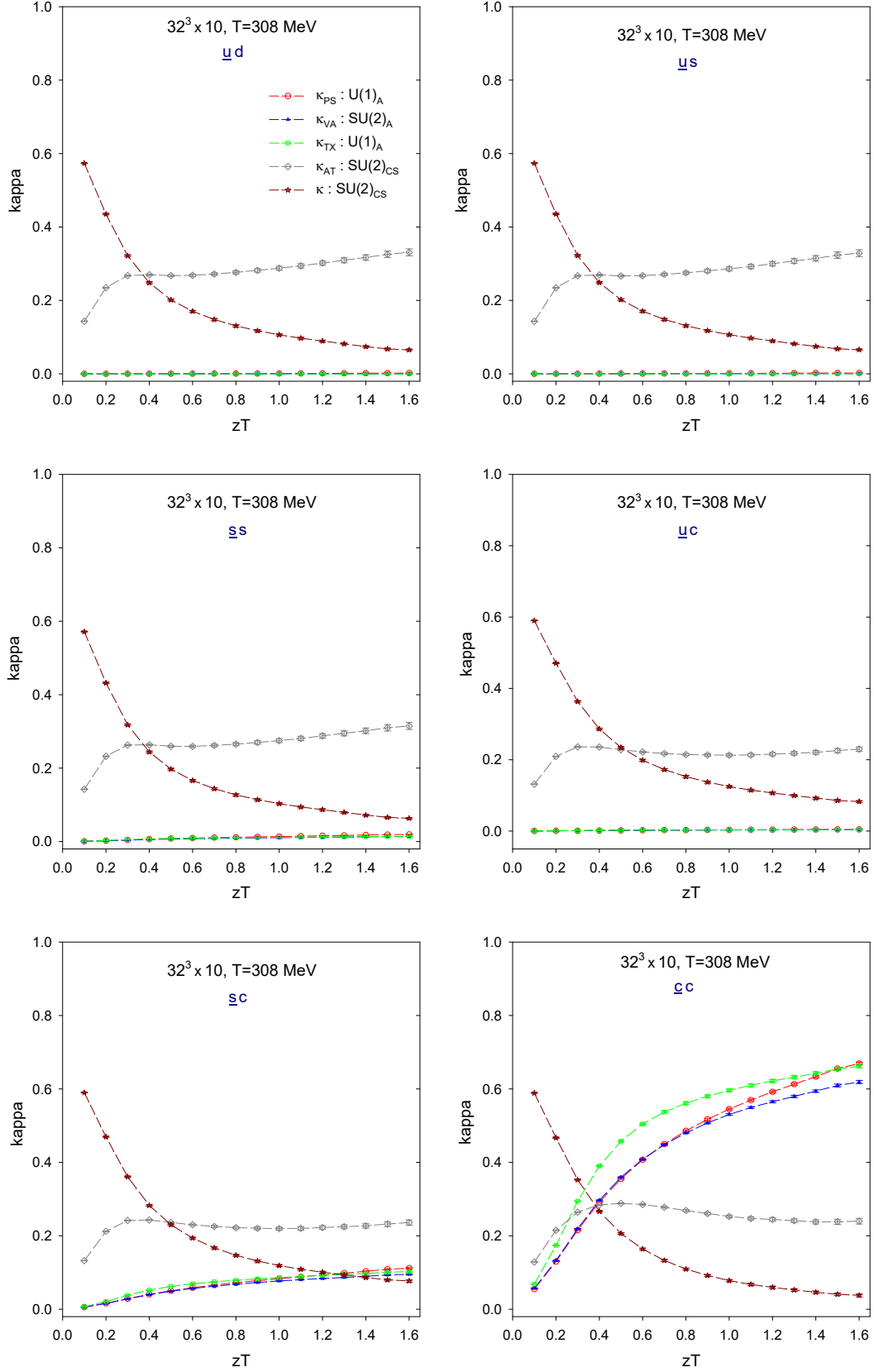
FIG. 11.   The symmetry breaking parameters of spatial z-correlators of meson interplotors of six flavor combinations ($\bar{u}d$, $\bar{u}s$, $\bar{s}s$, $\bar{u}c$, $\bar{s}c$, and $\bar{c}c$) in $N_f = 2 + 1 + 1$ lattice QCD at $T \simeq 385$ MeV.
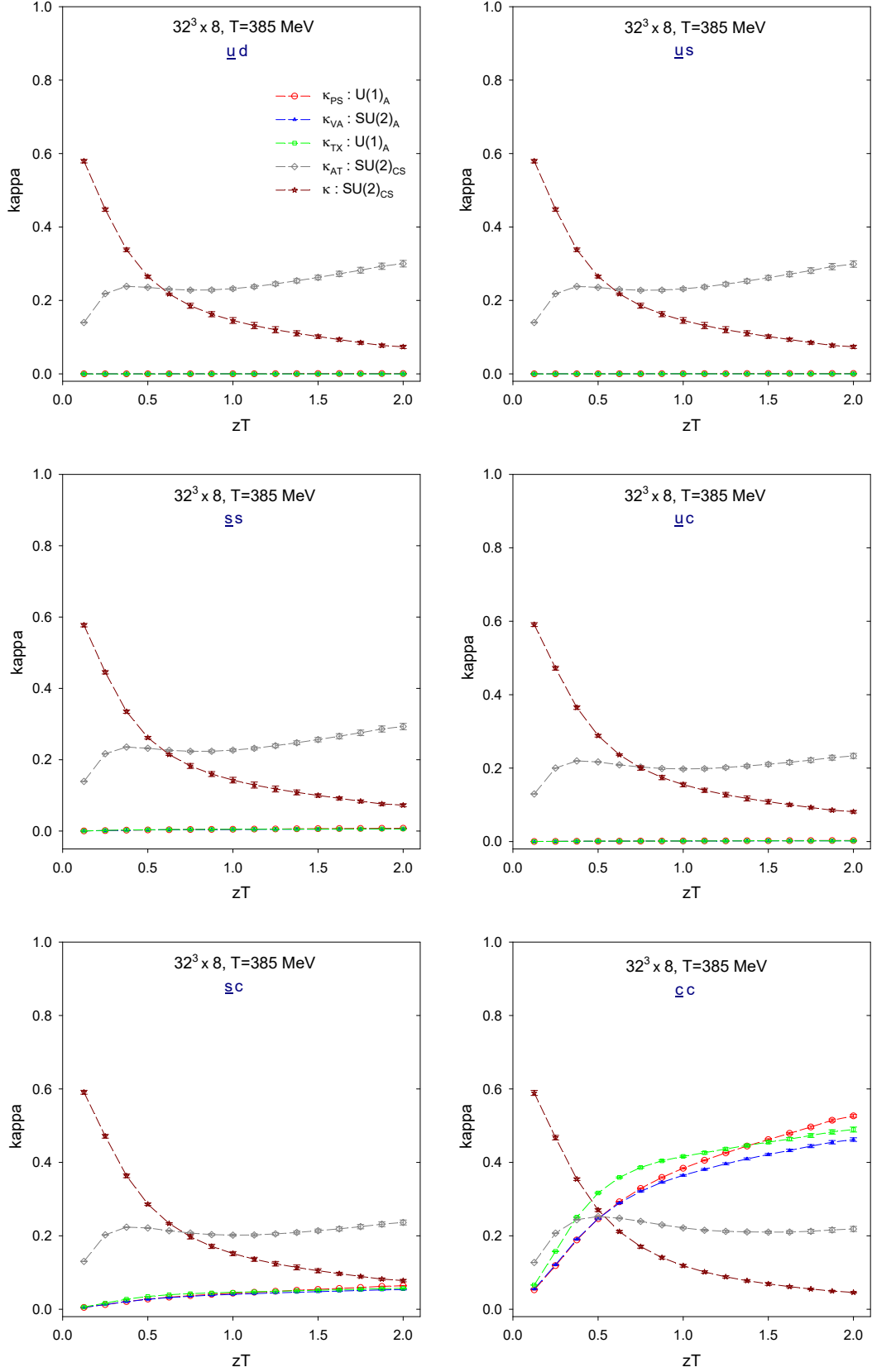
FIG. 12. The symmetry breaking parameters of spatial z-correlators of meson interplotors of six flavor combinations ($\bar{u}d$, $\bar{u}s$, $\bar{s}s$, $\bar{u}c$, $\bar{s}c$, and $\bar{c}c$) in $N_f = 2 + 1 + 1$ lattice QCD at $T \simeq 513$ MeV.
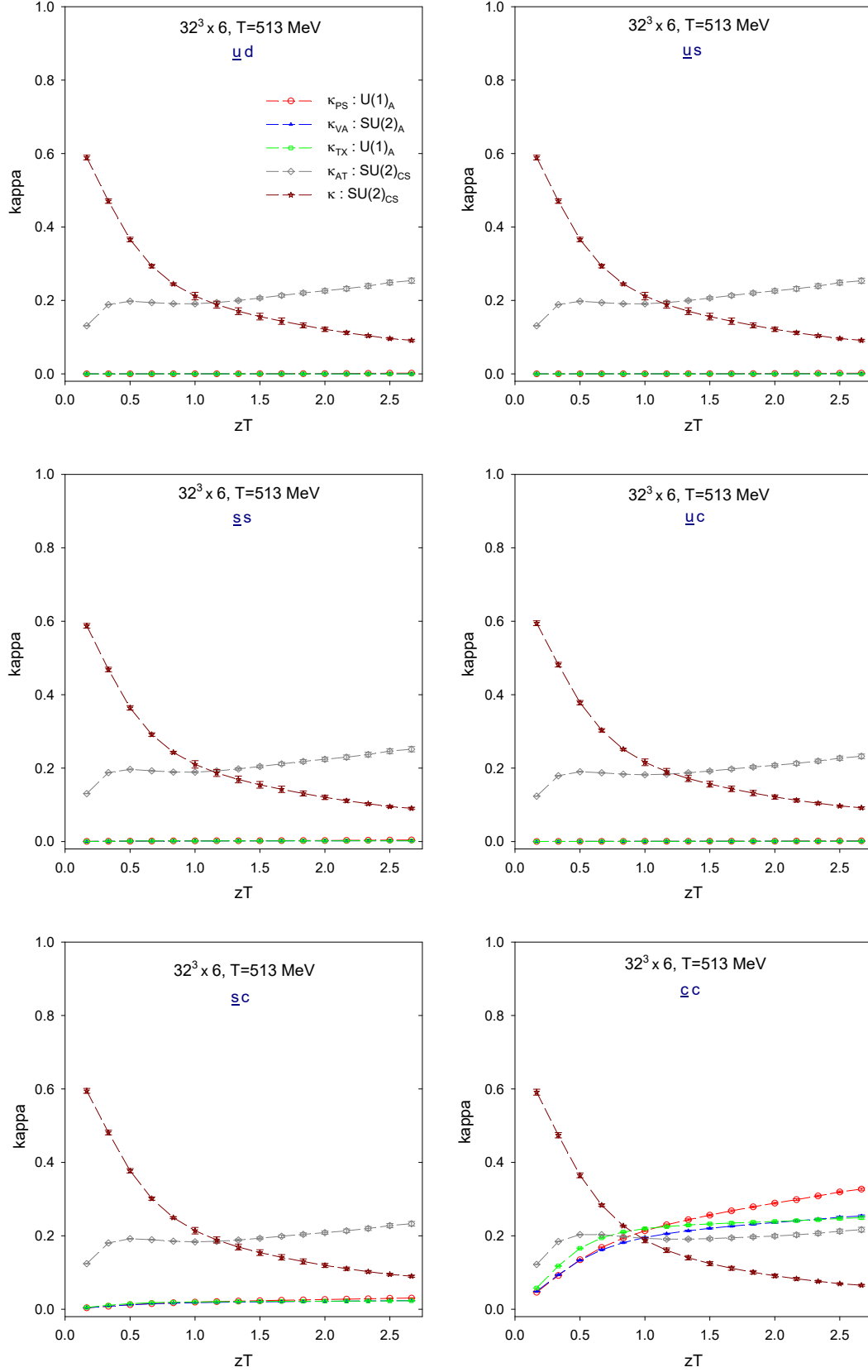
FIG. 13. The symmetry breaking parameters of spatial z-correlators of meson interplotors of six flavor combinations ($\bar{u}d$, $\bar{u}s$, $\bar{s}s$, $\bar{u}c$, $\bar{s}c$, and $\bar{c}c$) in $N_f = 2 + 1 + 1$ lattice QCD at $T \simeq 770$ MeV.
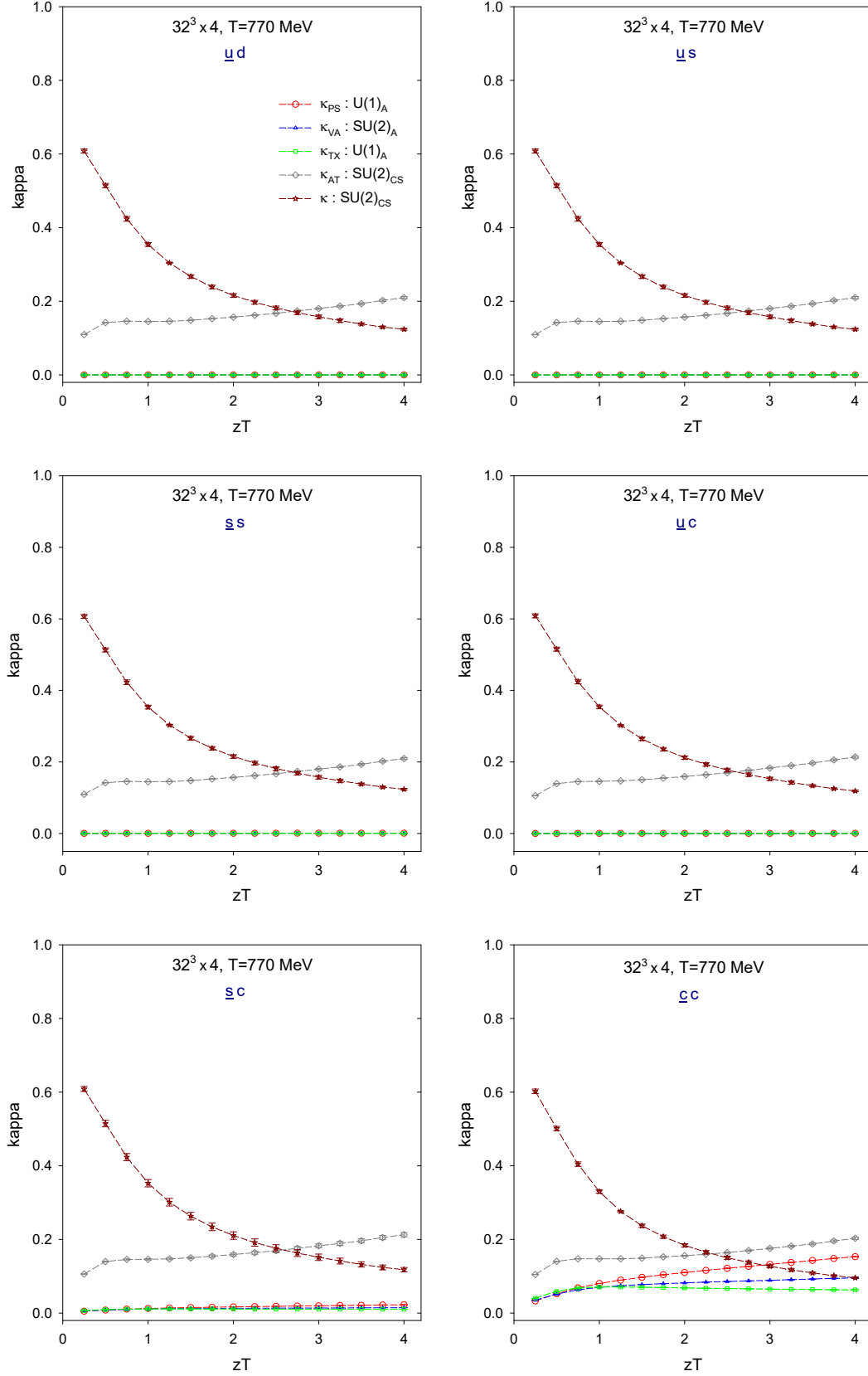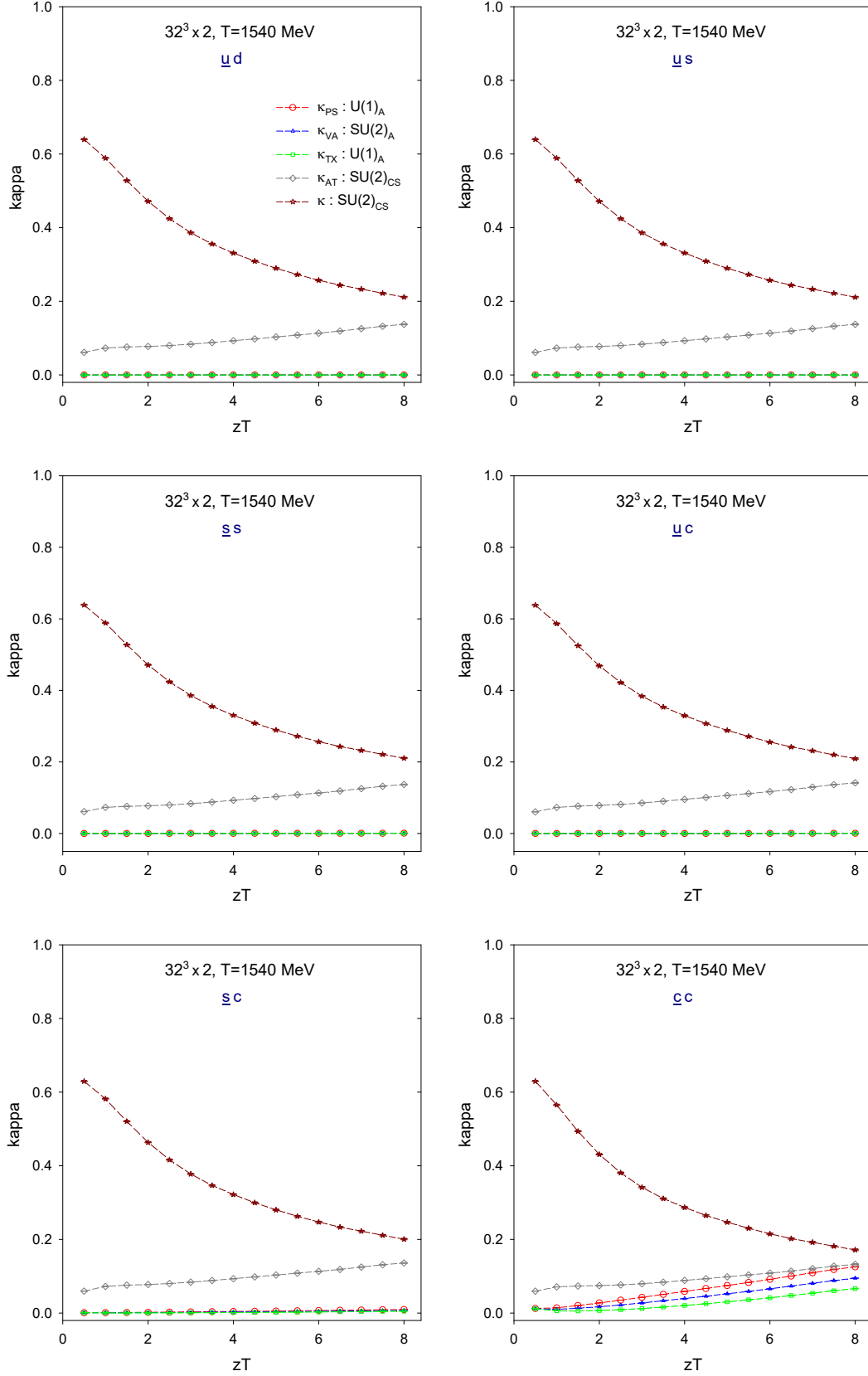
FIG. 14.   The symmetry breaking parameters of spatial z-correlators of meson interplotors of six flavor combinations ($\bar{u}d$, $\bar{u}s$, $\bar{s}s$, $\bar{u}c$, $\bar{s}c$, and $\bar{c}c$) in $N_f = 2 + 1 + 1$ lattice QCD at $T \simeq 1540$ MeV.

κ_{AT}, and κ, as defined in Sec. III.

In Figs. 8-14, the symmetry breaking parameters of six flavor combinations are plotted as a function of the dimensionless variable zT, for seven temperatures in the range of 190-1540 MeV.

At each T, and for fixed zT, the chiral symmetry breakings due to the quark masses of the meson operator can be seen clearly from κ_{VA}, κ_{PS}, and κ_{TX}, in the order of

$$\kappa_\alpha^{\bar{u}d} < \kappa_\alpha^{\bar{u}s} < \kappa_\alpha^{\bar{u}c} < \kappa_\alpha^{\bar{s}s} < \kappa_\alpha^{\bar{s}c} < \kappa_\alpha^{\bar{c}c} \tag{24}$$

for each channel of $\alpha = (VA, PS, TX)$. Also, for each flavor content, $\kappa_\alpha(zT)$ at fixed zT is a monotonic decreasing function of T. Note that for the charmonium $\bar{c}c$, the chiral symmetry breakings at $T = 1540$ are still not negligible, e.g., at $zT = 4$, $0.02 \lesssim \kappa_{TX} < \kappa_{VA} < \kappa_{PS} \lesssim 0.06$.

About the $SU(2)_{CS}$ symmetry breaking parameter $\kappa_{CS} = \max(\kappa_{AT}, \kappa_{TX})$, for any flavor combination, it is a monotonic decreasing function of T at fixed zT, since both $\kappa_{AT}(zT)$ and $\kappa_{TX}(zT)$ are monotonic decreasing function of T. However, the flavor dependence of κ_{CS} turns out to be rather nontrivial, and it is temperature dependent. Similarly, the flavor depenedence of the $SU(2)_{CS}$ symmetry fading parameter κ is also temperature dependent. Nevertheless, it is interesting to point out that κ_{CS} of the $\bar{u}c$ sector is the smallest among all flavor sectors, while κ is almost the same for all flavor sectors, for all seven temperatures in the range of 190-1540 MeV. This suggests that the most attractive vector meson channels to detect the emergence of approximate $SU(2)_{CS}$ symmetry are in the $\bar{u}c$ sector. This will be addressed more quantitatively in the subsection V B, in terms of the window of T for the approximate $SU(2)_{CS}$ symmetry.

A. Hierarchical restoration of chiral symmetries

Now we proceed to investigate the restoration of chiral symmetries in $N_f = 2+1+1$ lattice QCD at the physical point. We use the criteria (6) and (10) to obtain T_c and T_1 for each flavor combination. To this end, we collect the data of $\kappa_{VA}(zT)$ and $\kappa_{TX}(zT)$ at the same $zT = (0.5, 1, 2)$, and plot them as a function of T, as shown in Figs. 15 and 16. According to (24), it follows that for any ϵ_{VA} in (6) and any ϵ_{TX} in (10), the flavor dependence of T_c

FIG. 15. The $SU(2)_L \times SU(2)_R$ chiral symmetry breaking parameter κ_{VA} at $zT = (0.5, 1, 2)$, for seven temperatures in the range $T \sim 190 - 1540$ MeV and six flavor combinations ($\bar{u}d$, $\bar{u}s$, $\bar{s}s$, $\bar{u}c$, $\bar{s}c$, $\bar{c}c$).

FIG. 16. The $U(1)_A$ symmetry breaking parameter κ_{TX} at $zT = (0.5, 1, 2)$, for seven temperatures in the range $T \sim 190 - 1540$ MeV and six flavor combinations ($\bar{u}d$, $\bar{u}s$, $\bar{s}s$, $\bar{u}c$, $\bar{s}c$, $\bar{c}c$).
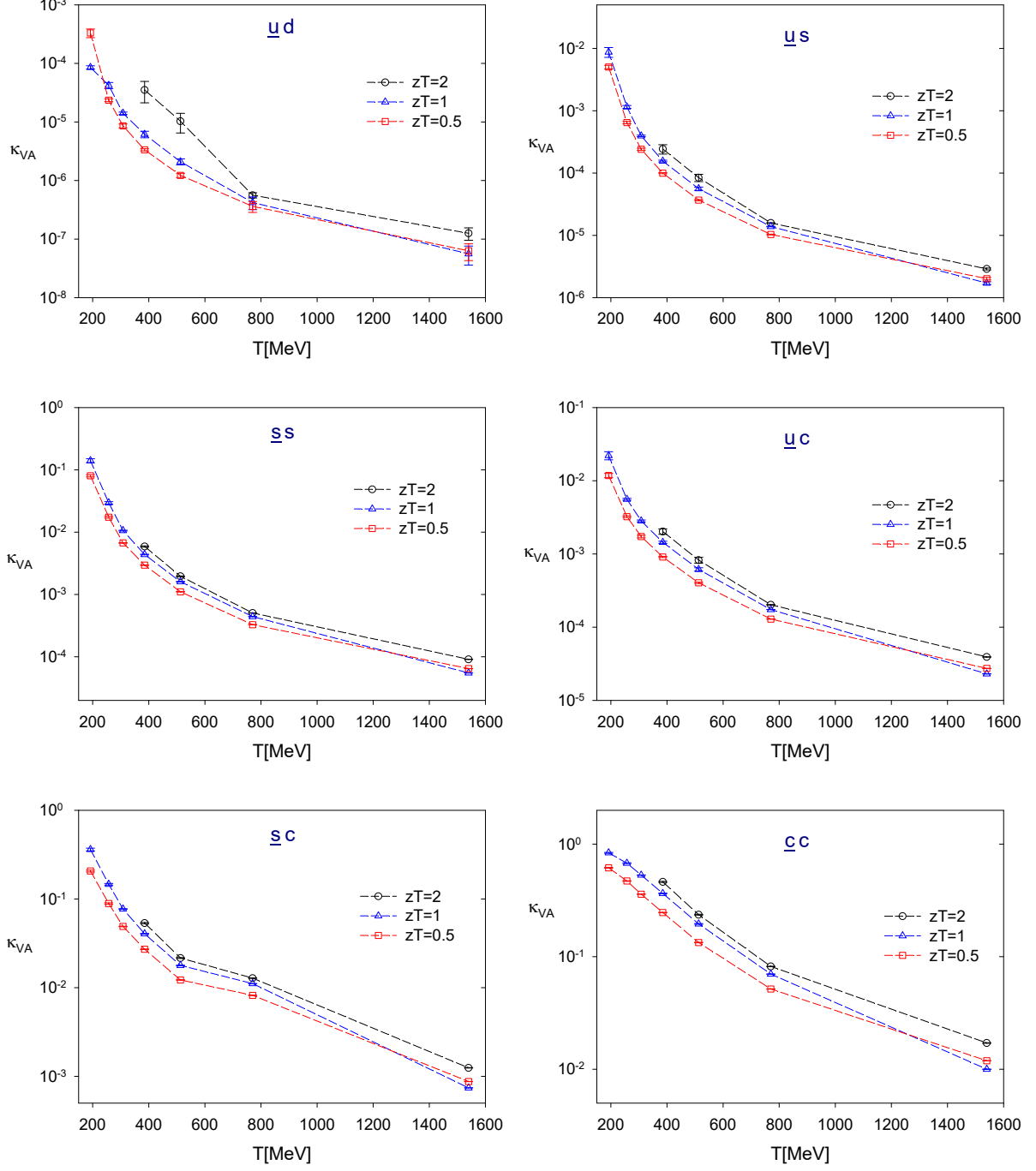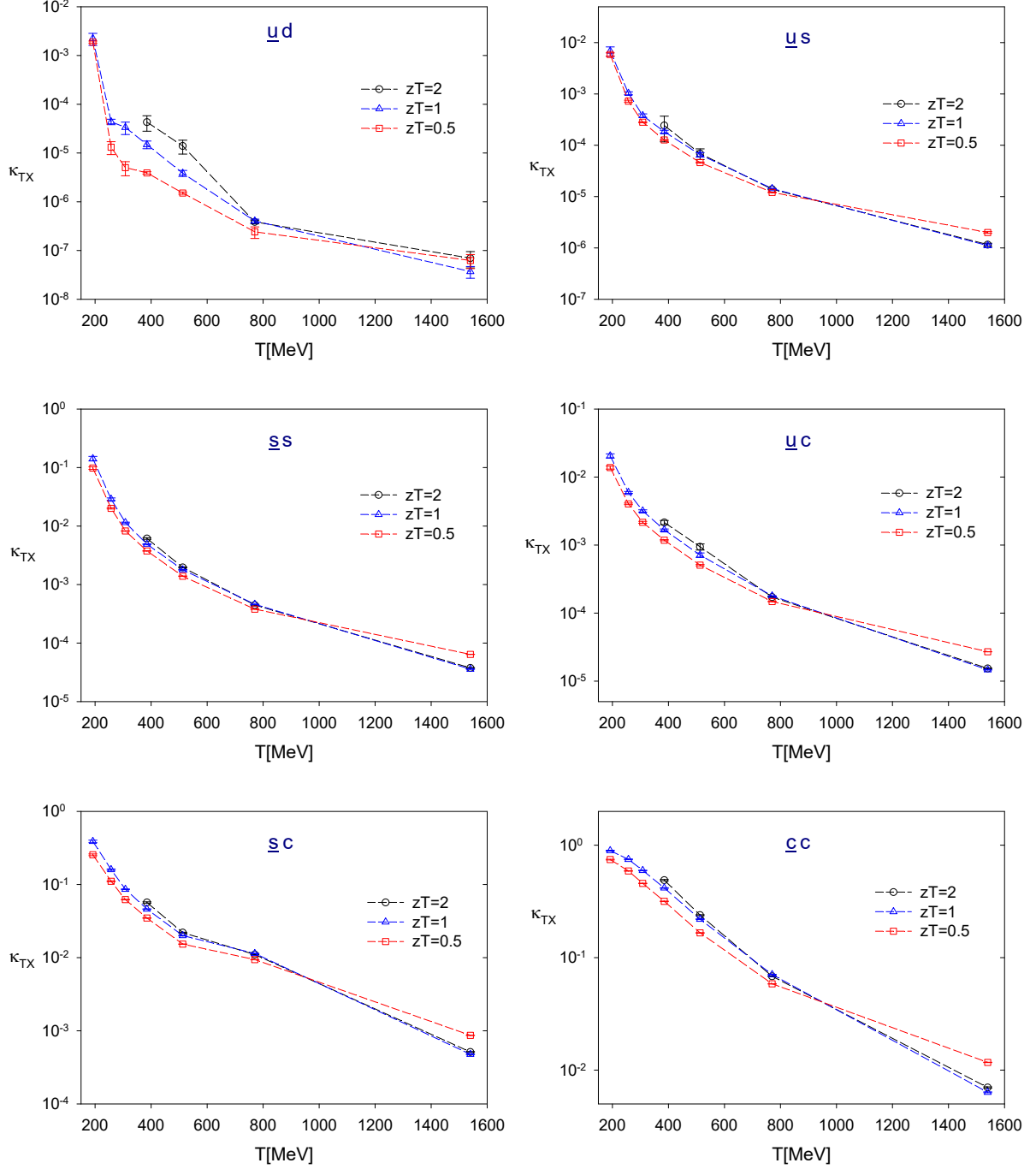

and T_1 is in the order of

$$T_c^{\bar{u}d} < T_c^{\bar{u}s} < T_c^{\bar{u}c} < T_c^{\bar{s}s} < T_c^{\bar{s}c} < T_c^{\bar{c}c}, \qquad (25)$$

$$T_1^{\bar{u}d} < T_1^{\bar{u}s} < T_1^{\bar{u}c} < T_1^{\bar{s}s} < T_1^{\bar{s}c} < T_1^{\bar{c}c}, \qquad (26)$$

33

which immididately gives

$$T_{c1}^{\bar{u}d} < T_{c1}^{\bar{u}s} < T_{c1}^{\bar{u}c} < T_{c1}^{\bar{s}s} < T_{c1}^{\bar{s}c} < T_{c1}^{\bar{c}c}. \tag{27}$$

Equations (25)-(27) are the first results of lattice QCD. They immediately give the hierarachic restoration of chiral symmetries in $N_f = 2 + 1 + 1$ QCD, i.e., from the restoration of $SU(2)_L \times SU(2)_R \times U(1)_A$ chiral symmetry of (u, d) quarks at $T_{c1}^{\bar{u}d}$ to the the restoration of $SU(3)_L \times SU(3)_R \times U(1)_A$ chiral symmetry of (u, d, s) quarks at $T_{c1}^{\bar{s}s} > T_{c1}^{\bar{u}d}$, then to the restoration of $SU(4)_L \times SU(4)_R \times U(1)_A$ chiral symmetry of (u, d, s, c) quarks at $T_{c1}^{\bar{c}c} > T_{c1}^{\bar{s}s}$.

In the following, we demonstrate the hierarchical restoration of chiral symmetries explicitly, for $\epsilon_{VA} = (0.05, 0.01)$ and $\epsilon_{TX} = (0.05, 0.01)$ respectively.

TABLE III. The temperature $T_c^{\bar{q}_1 q_2}$[MeV] satisfying the criterion (6) at $zT = (0.5, 1, 2)$, for $\epsilon_{VA} = (0.05, 0.01)$ respectively.

	$zT = 0.5$		$zT = 1$		$zT = 2$	
ϵ_{VA}	0.05	0.01	0.05	0.01	0.05	0.01
$T_c^{\bar{u}d}$	< 190	< 190	< 190	< 190	< 190	< 190
$T_c^{\bar{u}s}$	< 190	< 190	< 190	< 190	< 190	< 190
$T_c^{\bar{s}s}$	210(5)	285(5)	235(5)	315(5)	260(10)	345(10)
$T_c^{\bar{u}c}$	< 190	210(5)	< 190	230(5)	< 190	260(10)
$T_c^{\bar{s}c}$	305(5)	640(5)	360(5)	795(5)	395(5)	850(5)
$T_c^{\bar{c}c}$	785(5)	1640(10)	900(5)	1540(10)	990(5)	1785(10)

Using linear interpolotion or extrapolation of the data points in each figure of Figs. 15 and 16, we obtain the results of T_c and T_1 for six flavor combinations, as listed in the Tables III and IV, for $\epsilon_{VA} = (0.05, 0.01)$ and $\epsilon_{TX} = (0.05, 0.01)$ respectively.

In Tables III and IV, for both $\bar{u}d$ and $\bar{u}s$ sectors, both T_c and T_1 are less than 190 MeV, for any combinations of $\epsilon_{VA} = (0.05, 0.01)$, $\epsilon_{TX} = (0.05, 0.01)$, and $zT = (0.5, 1, 2)$. For these cases, $SU(2)_L \times SU(2)_R \times U(1)_A$ is restored at a temperature lower than 190 MeV, for both $\bar{u}d$ and $\bar{u}s$ sectors, However, for the $\bar{u}c$ sector, only for $\epsilon_{VA} = \epsilon_{TX} = 0.05$, $SU(2)_L \times SU(2)_R \times U(1)_A$ is restored at a temperature lower than 190 MeV.

34

TABLE IV. The temperature $T_1^{\bar{q}_1 q_2}$[MeV] satisfying the criterion (10) at $zT = (0.5, 1, 2)$, for $\epsilon_{TX} = (0.05, 0.01)$ respectively.

	$zT = 0.5$		$zT = 1$		$zT = 2$	
ϵ_{TX}	0.05	0.01	0.05	0.01	0.05	0.01
$T_1^{\bar{u}d}$	< 190	< 190	< 190	< 190	< 190	< 190
$T_1^{\bar{u}s}$	< 190	< 190	< 190	< 190	< 190	< 190
$T_1^{\bar{s}s}$	220(5)	295(5)	235(5)	320(5)	255(10)	350(10)
$T_1^{\bar{u}c}$	< 190	200(5)	< 190	230(5)	< 190	250(10)
$T_1^{\bar{s}c}$	335(5)	730(5)	375(5)	800(5)	400(5)	790(5)
$T_1^{\bar{c}c}$	835(5)	1610(10)	875(5)	1395(5)	865(5)	1420(5)

Now we investigate the hierarchical restoration of chiral symmetries with $\epsilon_{VA} = \epsilon_{TX} = 0.05$ and $zT = 1$. From Tables III and IV, one immediately sees that the $SU(3)_L \times SU(3)_R \times U(1)_A$ chiral symmetry of (u, d, s) quarks is restored at $T_c^{\bar{s}s} \simeq T_1^{\bar{s}s} \simeq 235(5)$ MeV, since T_c and T_1 of both $\bar{u}d$ and $\bar{u}s$ sectors are lower than 190 MeV. Moreover, for the $\bar{c}c$ sector, $T_c^{\bar{c}c} \simeq 900(5)$ MeV, $T_1^{\bar{c}c} \simeq 875(5)$ MeV, and T_c and T_1 of other flavor sectors are at lower temperatures, in the order of (25) and (26). Thus the $SU(4)_L \times SU(4)_R \times U(1)_A$ chiral symmetry of (u, d, s, c) quarks is restored at $T_{c1}^{\bar{c}c} \sim 900(5)$ MeV.

Next, we study how T_c (T_1) depends on ϵ_{VA} (ϵ_{TX}). Since $\kappa_{VA}^{\bar{q}_1 q_2} (\kappa_{TX}^{\bar{q}_1 q_2})$ at fixed zT is a monotonic decreasing function of T, it follows that T_c (T_1) is monotonically increased as ϵ_{VA} (ϵ_{TX}) is decreased (i.e., the precision of the chiral symmetry becomes higher). For example, if we set $\epsilon_{VA} = \epsilon_{TX} = 0.01$, then at $zT = 1$, the $SU(3)_L \times SU(3)_R \times U(1)_A$ chiral symmetry of (u, d, s) quarks is restored at $T_{c1}^{\bar{s}s} \simeq 320(5)$ MeV (since $T_c^{\bar{s}s} \lesssim T_1^{\bar{s}s} \simeq 320(5)$ MeV), and the $SU(4)_L \times SU(4)_R \times U(1)_A$ chiral symmetry of (u, d, s, c) quarks is restored at $T_{c1}^{\bar{c}c} \simeq 1540(10)$ MeV (since $T_c^{\bar{c}c} \simeq 1540(10)$ MeV and $T_1^{\bar{c}c} \simeq 1395(5)$ MeV). Obviously, no matter how small the values of ϵ_{VA} and ϵ_{TX} become, the hierarchical restoration of chiral symmetries in QCD with physical (u, d, s, c) quarks will occur at higher temperatures.

FIG. 17. The $SU(2)_{CS}$ symmetry breaking and fading parameters (κ_{AT}, κ) at $zT = (0.5, 1, 2)$, for flavor combinations $(\bar{u}d, \bar{u}s, \bar{s}s)$, and $T \sim 193 - 1540$ MeV.
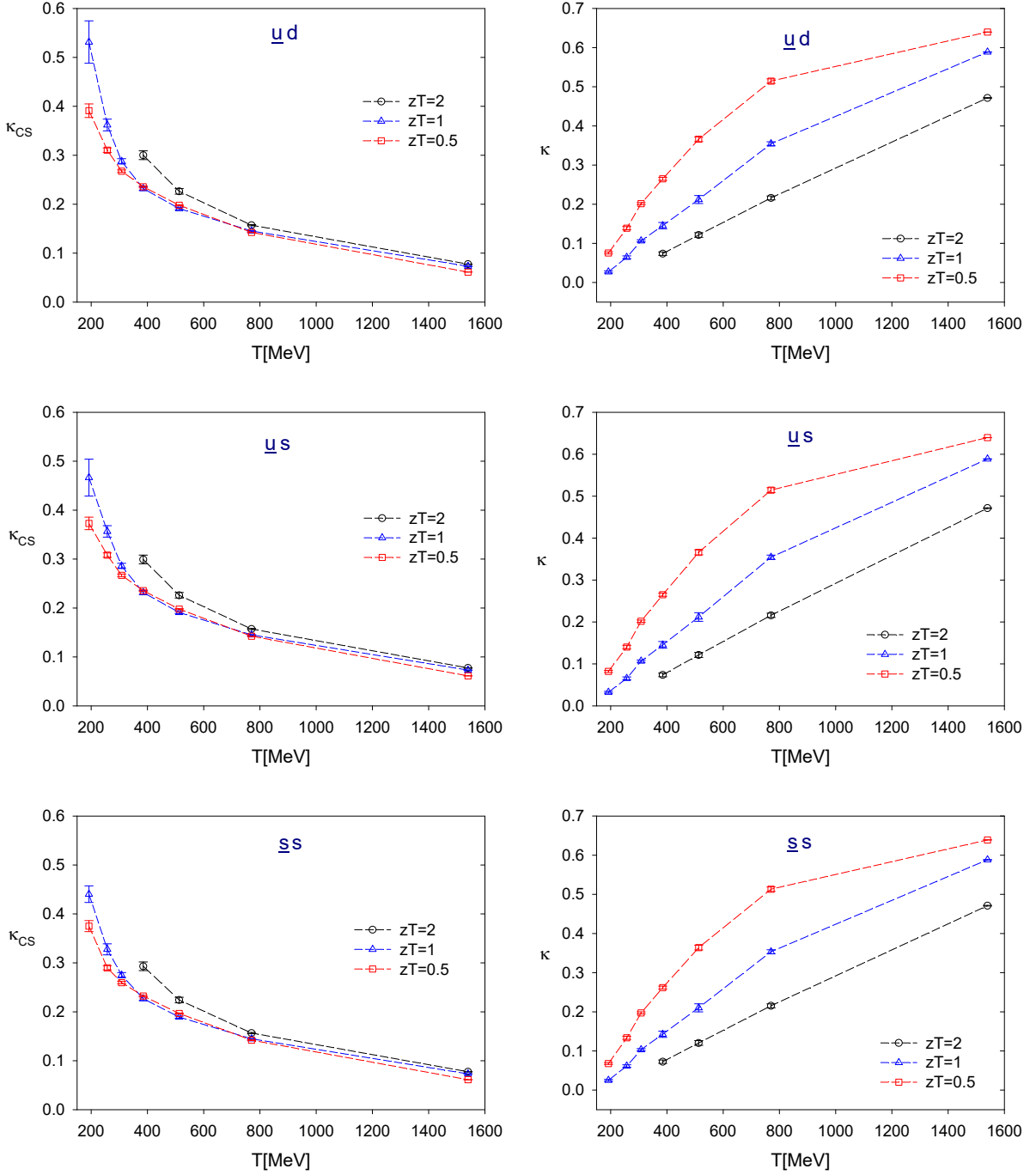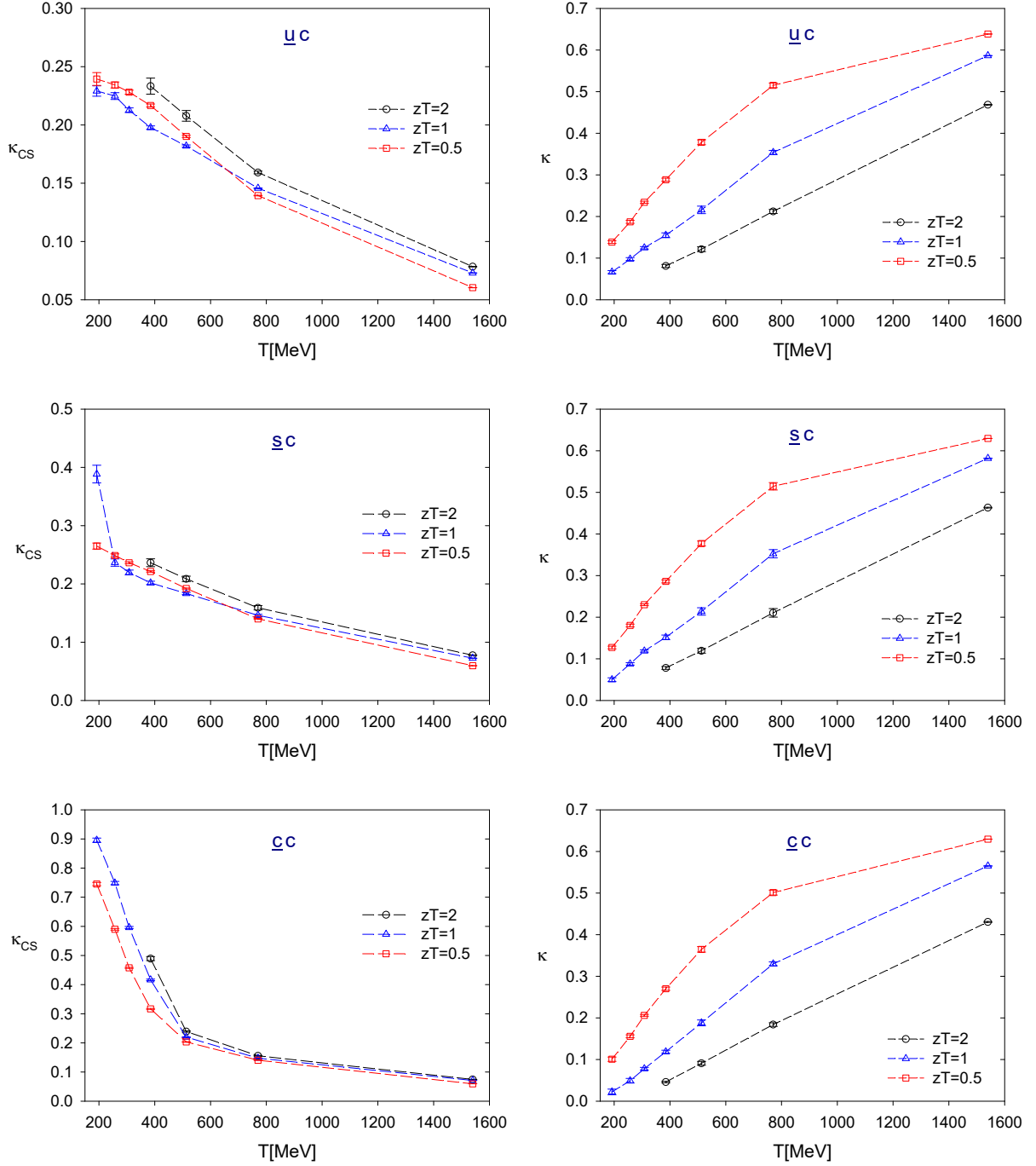
FIG. 18. The $SU(2)_{CS}$ symmetry breaking and fading parameters (κ_{AT}, κ) at $zT = (0.5, 1, 2)$, for flavor combinations $(\bar{u}c, \bar{s}c, \bar{c}c)$, and $T \sim 193 - 1540$ MeV.

B. $SU(2)_{\mathbf{CS}}$ **chiral-spin symmetry**

Next we study the approximate $SU(2)_{CS}$ symmetry of $N_f = 2 + 1 + 1$ lattice QCD at the physical point. We use the criterion (23) to determine the window of T of the approximate $SU(2)_{CS}$ symmetry, for six flavor combinations. To this end, we collect the data of $SU(2)_{CS}$ symmetry-breaking parameter $\kappa_{CS} = \max(\kappa_{AT}, \kappa_{TX})$ and symmetry-fading parameter κ at $zT = (0.5, 1, 2)$, and plot them as a function of T, in Figs. 17 and 18, for light mesons $(\bar{u}d, \bar{u}s, \bar{s}s)$ and heavy mesons $(\bar{u}c, \bar{s}c, \bar{c}c)$ respectively. In general, for any flavor content, at fixed zT, κ_{CS} is a monotonic decreasing function of T, while κ is a monotonic increasing function of T. Thus, for any ϵ_{cs} and ϵ_{fcs}, the window of T satisfying the criterion (23) can be determined. Note that, if ϵ_{cs} or ϵ_{fcs} becomes too small, the window of T would shrink to zero (null). Using linear interpolotion and extrapolation of the data points in Figs. 17 and 18, we obtain the results of T window in Tables V-VI at $zT = (1, 2)$ respectively, each for six flavor combinations, and for all combinations of ϵ_{cs} and ϵ_{fcs} sampling from $(0.1, 0.15, 0.20, 0.25, 0.30)$. For visual comparison, we plot the windows of T in Fig. 19, for a range of values of $(\epsilon_{cs}, \epsilon_{fcs})$ from large to small ones. Tables V-VI and Fig. 19 are the first results of lattice QCD.

It is interesting to see that the T windows of the approximate $SU(2)_{CS}$ symmetry are dominated by the channels of heavy vector mesons of $(\bar{u}c, \bar{s}c, \bar{c}c)$. As the precision of $SU(2)_{CS}$ symmetry gets higher with smaller ϵ_{cs} or ϵ_{fcs}, the T windows of the light vector mesons $(\bar{u}d, \bar{u}s, \bar{s}s)$ shrink to zero, only those of heavy vector mesons survive. This suggests that the most attractive vector meson channels to detect the emergence of approximate $SU(2)_{CS}$ symmetry are in the $(\bar{u}c, \bar{s}c, \bar{c}c)$ sectors, which may have phenomenological implications to the observation of the approximate $SU(2)_{CS}$ symmetry in relativistic heavy ion collision experiments such as those at LHC and RHIC. Moreover, the results of Tables V-VI and Fig. 19 also suggest that the hadron-like objects, in particular, in the channels of vector mesons with c quark, are likely to be predominantly bound by the chromoelectric interactions into color singlets at the temperatures inside their T windows of the approximate $SU(2)_{CS}$ symmetry, since the noninteracting theory with free quarks does not possess the $SU(2)_{CS}$ symmetry at all.

TABLE V. The approximate ranges of T satisfying the criterion (23) at $zT = 1$ for six flavor contents. The table lists all nonzero windows of T for all possible combinations of ϵ_{cs} and ϵ_{fcs} sampling from $(0.1, 0.15, 0.20, 0.25, 0.30)$. Each T window is in units of MeV, with uncertainties ± 5 MeV on both ends of the window.

ϵ_{cs}	ϵ_{fcs}	$\bar{u}d$	$\bar{u}s$	$\bar{s}s$	$\bar{u}c$	$\bar{s}c$	$\bar{c}c$
0.30	0.30	300-670	300-670	285-675	190-670	230-675	455-715
0.30	0.25	300-580	300-580	285-585	190-580	230-580	455-625
0.25	0.30	360-670	355-670	350-675	190-670	250-675	485-715
0.25	0.25	360-580	355-580	350-585	190-580	250-580	485-625
0.30	0.20	300-495	300-495	285-495	190-480	230-485	455-530
0.20	0.30	480-670	485-670	475-675	370-670	385-675	535-715
0.25	0.20	360-495	355-495	350-495	190-480	250-485	485-530
0.20	0.25	480-580	485-580	475-585	370-580	385-580	535-625
0.30	0.15	300-400	300-400	285-400	190-370	230-380	NULL
0.25	0.15	360-400	355-400	350-400	190-370	250-380	NULL
0.20	0.20	480-495	485-495	475-495	370-480	385-485	NULL
0.30	0.10	NULL	NULL	285-310	190-260	230-280	NULL
0.25	0.10	NULL	NULL	NULL	190-260	250-280	NULL

VI.   Concluding remarks

In this study, we have generated seven gauge ensembles of $N_f = 2+1+1$ lattice QCD with $(u/d, s, c)$ optimal domain-wall quarks at the physical point, on the $32^3 \times (16, 12, 10, 8, 6, 4, 2)$ lattices with lattice spacing $a \sim 0.064$ fm, for seven temperatures in the range of 190-1540 MeV, as summarized in Table I. Our plan is to complete 21 gauge ensembles with three lattice spacings $a \sim (0.064, 0.069, 0.075)$ fm, which can be used to extract the continuum limit of the observables, for temperatures in the range of 160-1540 MeV.

Using seven gauge ensembles with $a \sim 0.064$ fm, we computed the meson z-correlators for the complete set of Dirac bilinears (scalar, pseudoscalar, vector, axial vector, tensor vector, and axial-tensor vector), and each for six combinations of quark flavors ($\bar{u}d$, $\bar{u}s$, $\bar{s}s$, $\bar{u}c$, $\bar{s}c$,

39

TABLE VI. The approximate ranges of T satisfying the criterion (23) at $zT = 2$ for six flavor contents. The table lists all nonzero windows of T for all possible combinations of ϵ_{cs} and ϵ_{fcs} sampling from $(0.1, 0.15, 0.20, 0.25, 0.30)$. Each T window is in units of MeV, with uncertainties ± 5 MeV on both ends of the window.

| ϵ_{cs}	ϵ_{fcs}	$\bar{u}d$	$\bar{u}s$	$\bar{s}s$	$\bar{u}c$	$\bar{s}c$	$\bar{c}c$
0.30	0.30	385-1030	385-1030	370-1030	190-1035	190-1045	470-1130
0.30	0.25	385-875	385-875	370-875	190-880	190-895	470-975
0.30	0.20	385-730	385-730	370-730	190-735	190-740	470-820
0.30	0.15	385-590	385-590	370-595	190-595	190-600	470-670
0.30	0.10	385-455	385-455	370-460	190-440	190-455	470-535
0.25	0.30	470-1030	470-1030	465-1030	250-1035	330-1045	505-1130
0.25	0.25	470-875	470-875	465-875	250-880	330-895	505-975
0.25	0.20	470-730	470-730	465-730	250-735	330-740	505-820
0.25	0.15	470-590	470-590	465-595	250-595	330-600	505-670
0.20	0.30	610-1030	610-1030	610-1030	550-1035	555-1045	555-1130
0.20	0.25	610-875	610-875	610-875	550-880	555-895	555-975
0.20	0.20	610-730	610-730	610-730	550-735	555-740	555-820
0.15	0.30	825-1030	830-1030	830-1030	855-1035	850-1045	820-1130
0.15	0.25	825-875	830-875	830-875	855-880	850-895	820-975
0.25	0.10	NULL	NULL	NULL	250-440	330-455	505-535
0.20	0.15	NULL	NULL	NULL	550-595	555-600	555-670
0.15	0.20	NULL	NULL	NULL	NULL	NULL	NULL

$\bar{c}c$). Then we use the criteria (6) and (10) to determine T_c and T_1 for each flavor combination, and obtain the hierarchy of restoration of chiral symmetries, in the order of

$$T_c^{\bar{u}d} < T_c^{\bar{u}s} < T_c^{\bar{u}c} < T_c^{\bar{s}s} < T_c^{\bar{s}c} < T_c^{\bar{c}c},$$
$$T_1^{\bar{u}d} < T_1^{\bar{u}s} < T_1^{\bar{u}c} < T_1^{\bar{s}s} < T_1^{\bar{s}c} < T_1^{\bar{c}c}.$$

These are the first results in lattice QCD. They immediately give the the hierarchical restoration of chiral symmetries in $N_f = 2 + 1 + 1$ QCD, i.e., from the restoration of $SU(2)_L \times SU(2)_R \times U(1)_A$ chiral symmetry of (u, d) quarks at $T_{c1}^{\bar{u}d}$ to the restoration of

FIG. 19.   The windows of T satisfying the criterion (23) for the $SU(2)_{CS}$ symmetry are plotted for six flavor contents and a range of $(\epsilon_{cs}, \epsilon_{fcs})$, according to the data in Tables V-VI.
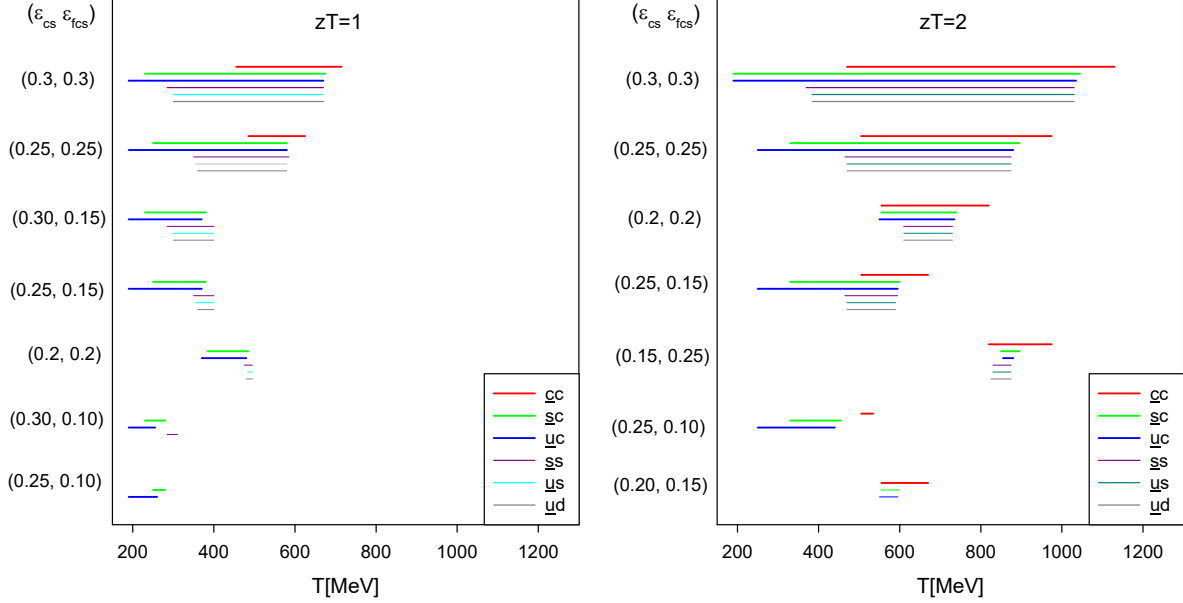
$SU(3)_L \times SU(3)_R \times U(1)_A$ chiral symmetry of (u, d, s) quarks at $T_{c1}^{\bar{s}s} > T_{c1}^{\bar{u}d}$, then to the restoration of $SU(4)_L \times SU(4)_R \times U(1)_A$ chiral symmetry of (u, d, s, c) quarks at $T_{c1}^{\bar{c}c} > T_{c1}^{\bar{s}s}$.

Obviously, the hierarchical restoration of chiral symmetries is expected to be realized in QCD with physical (u, d, s, c, b) quarks, adding the restoration of $SU(5)_L \times SU(5)_R \times U(1)_A$ chiral symmetry of (u, d, s, c, b) quarks at $T_{c1}^{\bar{b}b} > T_{c1}^{\bar{c}c}$. We will study the restoration of chiral symmetries in $N_f = 2+1+1+1$ lattice QCD with physical s, c and b quarks, but unphysical u/d quarks with $M_{\pi^{\pm}} \sim 700$ MeV [17], for eight ensembles with temperatures in the range of 300-3250 MeV, on $40^3 \times (20, 16, 12, 10, 8, 6, 4, 2)$ lattices with lattice spacing $a \sim 0.03$ fm.

In this work, we observe that for mesons with quark contents $(\bar{q}q, \bar{q}Q, \bar{Q}Q)$ and $m_q < m_Q$ in $N_f = 2+1+1$ QCD, the temperatures of the restoration of $SU(2)_L \times SU(2)_R \times U(1)_A$ chiral symmetry in these three sectors satisfy the hierarchy:

$$T_{c1}^{\bar{q}q} \leq T_{c1}^{\bar{q}Q} \leq T_{c1}^{\bar{Q}Q}, \quad m_q < m_Q.$$

However, we do not know the hierarchy of T_{c1} for mesons involving more than two quarks. For example, for three quarks (q_1, q_2, q_3) with $m_1 < m_2 < m_3$, we do not know whether

41

$T_{c1}^{\bar{q}_1 q_3} < T_{c1}^{\bar{q}_2 q_2}$ or vice versa. In reality, for physical (u, s, c) quarks, we observe that

$$T_{c1}^{\bar{q}_1 q_3} < T_{c1}^{\bar{q}_2 q_2}. \tag{28}$$

Yet, in general, it is unclear to what extent (28) depends on the ratios of quark masses.

One of the phenomenological implications of the hierarchical restoration of chiral symmetries is the pattern of hadron dissolution at high temperatures, which leads to the hierarchical dissolution of hadrons, and the hierarchical suppression of hadrons in the quark-gluon plasma. Theoretically, the meson with quark content $\bar{q}Q$ dissolves completely as $\bar{q}$ and Q become deconfined, i.e., when the screening mass of $\bar{q}Q$ is larger than its counterpart in the noninteracting theory with free quarks of the same masses. Presumably, $m_{\text{scr}}^{\bar{q}Q} \geq m_{\text{scr}}^{\bar{q}Q(\text{free})}$ happens at the temperature $T_d^{\bar{q}Q} \gtrsim T_{c1}^{\bar{q}Q}$, after the $SU(2)_L \times SU(2)_R \times U(1)_A$ chiral symmetry of $\bar{q}\Gamma Q$ has been effectively restored. Thus, for $N_f = 2 + 1 + 1$ lattice QCD at the physical point, one expects that the hierarchy of dissolution of mesons is exactly the same as that of the restoration of chiral symmetries (27), i.e.,

$$T_d^{\bar{u}d} < T_d^{\bar{u}s} < T_d^{\bar{u}c} < T_d^{\bar{s}s} < T_d^{\bar{s}c} < T_d^{\bar{c}c}. \tag{29}$$

This leads to the hierarchical suppression of mesons in quark-gluon plasma, which could be observed in the relativistic heavy ion collision experiments such as those at LHC and RHIC. Here we recall the seminal paper by Matusi and Satz [18], in which it was proposed that the dissolution of J/ψ in the quark-gluon plasma would result in the suppression of their production in heavy ion collision experiments. To investigate whether (29) holds in $N_f = 2 + 1 + 1$ lattice QCD at the physical point is beyond the scope of this paper.

Besides the meson z-correlators, the restoration of chiral symmetry in high temperature QCD can also be observed in the baryon z-correlators [2]. For QCD with $N_f = 2(3)$ massless quarks, the chiral multiplets of baryon operators have been obtained by the group theoretical methods, see e.g., Ref. [19] and the references therein. Now, for QCD with physical (u, d, s, c, b) quarks, with quark masses ranging from a few MeV to a few GeV, we expect that the hierarchical restoration of chiral symmetries can be observed from the degeneracies of z-correlators of baryon chiral multiplets. It would be interesting to see whether the hierachy of chiral symmetry restoration from the baryon z-correlators is compatible with that from the meson z-correlators.

About the approximate $SU(2)_{CS}$ chiral spin symmetry, it is interesting to see that the T windows satisfying the criterion (23) are dominated by the the channels of heavy vector mesons with flavor contents $(\bar{u}c, \bar{s}c, \bar{c}c)$, as shown in Tables V-VI and Fig. 19. These are the first results of lattice QCD. They suggest that the hadron-like objects, in particular, in the channels of vector mesons with c quark, at the temperatures inside their T windows, are likely to be predominantly bound by the chromoelectric interactions into color singlets, since the noninteracting theory with free quarks does not possess the $SU(2)_{CS}$ symmetry at all. Moreover, they provide hints to look for the approximate emergent $SU(2)_{CS}$ symmetry in the relativistic heavy ion collision experiments such as those at LHC and RHIC, e.g., to focus on the channels of vector mesons with c quark.

Obviously, it is interesting to find out the T windows of the approximate $SU(2)_{CS}$ symmetry for heavy vector mesons involving the b quark, in lattice QCD with (u, d, s, c, b) quarks. To this end, we will investigate the approximate $SU(2)_{CS}$ symmetry in $N_f = 2 + 1 + 1 + 1$ lattice QCD with physical s, c and b quarks, but unphysical u/d quarks with $M_{\pi^\pm} \sim 700$ MeV [17], for eight ensembles with temperatures in the range of 300-3250 MeV, on $40^3 \times (20, 16, 12, 10, 8, 6, 4, 2)$ lattices with lattice spacing $a \sim 0.03$ fm.

Finally, it is necessary to clarify the nature of these meson-like objects in the $J = 1$ channels (i.e., V_k, A_k, T_k, and X_k) which are relevant to the approximate $SU(2)_{CS}$ symmetry, for all six flavor contents $(\bar{u}d, \bar{u}s, \bar{s}s, \bar{u}c, \bar{s}c, \bar{c}c)$, by examining how their spectral functions evolve as T is increased. If bound-state peaks exist in the T windows of the approximate $SU(2)_{CS}$ symmetry, and also the widths of these peaks gradually broaden as T is increased, and the peaks eventually disappear as T is increased above the windows, then the degrees of freedom in these meson-like objects can be asserted to be color-singlet (melting) mesons rather than deconfined quarks and gluons. To this end, one may consider the approach of Refs. [20–22] for $J = 0$ mesons, and generalize it to $J = 1$ mesons. Also, the spatial z-correlators of vector mesons have to be evaluated to high precision even at large distances such that the damping factor $D_{m,\beta}(\vec{u})$ [21] of each $J = 1$ meson channel can be extracted reliably. The proposed prescription in Ref. [1] provides a viable way to attain this goal.

Acknowledgement

---

[1] T. W. Chiu, "Symmetries of meson correlators in high-temperature QCD with physical (u/d,s,c) domain-wall quarks," Phys. Rev. D **107**, no.11, 114501 (2023) [arXiv:2302.06073 [hep-lat]].

[2] C. E. DeTar and J. B. Kogut, "The Hadronic Spectrum of the Quark Plasma," Phys. Rev. Lett. **59**, 399 (1987); "Measuring the Hadronic Spectrum of the Quark Plasma," Phys. Rev. D **36**, 2828 (1987)

[3] A. Bazavov, S. Dentinger, H. T. Ding, P. Hegde, O. Kaczmarek, F. Karsch, E. Laermann, A. Lahiri, S. Mukherjee and H. Ohno, *et al.* "Meson screening masses in (2+1)-flavor QCD," Phys. Rev. D **100**, no.9, 094510 (2019) [arXiv:1908.09552 [hep-lat]].

[4] N. J. Evans, S. D. H. Hsu and M. Schwetz, "Topological charge and U(1)-A symmetry in the high temperature phase of QCD," Phys. Lett. B **375**, 262-266 (1996) Phys. Lett. B **375**, 262-266 (1996) [arXiv:hep-ph/9601361 [hep-ph]].

[5] M. C. Birse, T. D. Cohen and J. A. McGovern, "U(1)-A symmetry and correlation functions in the high temperature phase of QCD," Phys. Lett. B **388**, 137-140 (1996) [arXiv:hep-ph/9608255 [hep-ph]].

[6] L. Y. Glozman, "SU(4) symmetry of the dynamical QCD string and genesis of hadron spectra, Eur. Phys. J. A **51**, no.3, 27 (2015) [arXiv:1407.2798 [hep-ph]].

[7] L. Y. Glozman and M. Pak, "Exploring a new SU(4) symmetry of meson interpolators," Phys. Rev. D **92**, no.1, 016001 (2015) [arXiv:1504.02323 [hep-lat]].

[8] C. Rohrhofer, Y. Aoki, G. Cossu, H. Fukaya, C. Gattringer, L. Y. Glozman, S. Hashimoto, C. B. Lang and S. Prelovsek, "Symmetries of spatial meson correlators in high temperature QCD," Phys. Rev. D **100**, no.1, 014502 (2019) [arXiv:1902.03191 [hep-lat]].

[9] T. W. Chiu, "Optimal domain wall fermions," Phys. Rev. Lett. **90**, 071601 (2003) [hep-lat/0209153]; "Domain-Wall Fermion with R_5 Symmetry," Phys. Lett. B **744**, 95 (2015) [arXiv:1503.01750 [hep-lat]].

[10] T. W. Chiu, T. H. Hsieh, Y. Y. Mao [TWQCD Collaboration], "Pseudoscalar Meson in Two Flavors QCD with the Optimal Domain-Wall Fermion," Phys. Lett. B **717**, 420 (2012) [arXiv:1109.3675 [hep-lat]].

[11] Y. C. Chen, T. W. Chiu [TWQCD Collaboration], "Exact Pseudofermion Action for Monte Carlo Simulation of Domain-Wall Fermion," Phys. Lett. B **738**, 55 (2014) [arXiv:1403.1683 [hep-lat]].

[12] Y. C. Chen, T. W. Chiu and T. H. Hsieh [TWQCD Collaboration], "Topological susceptibility in finite temperature QCD with physical (u/d,s,c) domain-wall quarks," Phys. Rev. D **106**, no.7, 074501 (2022) [arXiv:2204.01556 [hep-lat]].

[13] R. Narayanan and H. Neuberger, "Infinite N phase transitions in continuum Wilson loop operators," JHEP **0603**, 064 (2006) [hep-th/0601210].

[14] M. Luscher, "Properties and uses of the Wilson flow in lattice QCD," JHEP **1008**, 071 (2010); Erratum: [JHEP **1403**, 092 (2014)] [arXiv:1006.4518 [hep-lat]].

[15] A. Bazavov *et al.* [MILC Collaboration], "Gradient flow and scale setting on MILC HISQ ensembles," Phys. Rev. D **93**, no. 9, 094510 (2016) [arXiv:1503.02769 [hep-lat]].

[16] Y. C. Chen, T. W. Chiu [TWQCD Collaboration], "Chiral Symmetry and the Residual Mass in Lattice QCD with the Optimal Domain-Wall Fermion," Phys. Rev. D **86**, 094508 (2012) [arXiv:1205.6151 [hep-lat]].

[17] T. W. Chiu, "Beauty mesons in N_f=2+1+1+1 lattice QCD with exact chiral symmetry," Phys. Rev. D **102**, no.3, 034510 (2020) [arXiv:2004.02142 [hep-lat]].

[18] T. Matsui and H. Satz, "J/ψ Suppression by Quark-Gluon Plasma Formation," Phys. Lett. B **178**, 416-422 (1986)

[19] T. D. Cohen and X. D. Ji, "Chiral multiplets of hadron currents," Phys. Rev. D **55**, 6870-6876 (1997) [arXiv:hep-ph/9612302 [hep-ph]].

[20] J. Bros and D. Buchholz, "Particles and propagators in relativistic thermo field theory," Z. Phys. C **55**, 509-514 (1992)

[21] J. Bros and D. Buchholz, "Asymptotic dynamics of thermal quantum fields," Nucl. Phys. B **627**, 289-310 (2002) [arXiv:hep-ph/0109136 [hep-ph]].

[22] P. Lowdon and O. Philipsen, "Pion spectral properties above the chiral crossover of QCD," JHEP **10**, 161 (2022) [arXiv:2207.14718 [hep-lat]].